Accepted Manuscript

New 1,5 and 2,5-disubstituted tetrazoles-dependent activity towards surface barrier of *Candida albicans*

Monika Staniszewska, Małgorzata Gizińska, Ewa Mikulak, Klaudia Adamus, Mirosława Koronkiewicz, Edyta Łukowska-Chojnacka

PII: S0223-5234(17)30992-3

DOI: 10.1016/j.ejmech.2017.11.089

Reference: EJMECH 9964

To appear in: *European Journal of Medicinal Chemistry*

Received Date: 22 August 2017

Revised Date: 13 November 2017

Accepted Date: 28 November 2017

Please cite this article as: M. Staniszewska, Mał. Gizińska, E. Mikulak, K. Adamus, Mirosł. Koronkiewicz, E. Łukowska-Chojnacka, New 1,5 and 2,5-disubstituted tetrazoles-dependent activity towards surface barrier of *Candida albicans*, *European Journal of Medicinal Chemistry* (2018), doi: 10.1016/j.ejmech.2017.11.089.

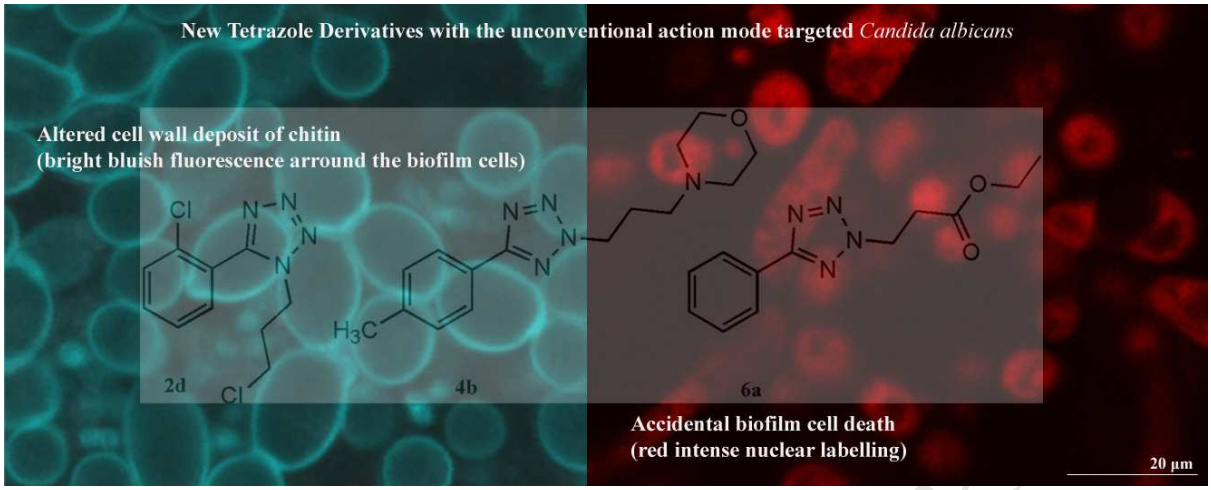

Title:

New 1,5 and 2,5-Disubstituted Tetrazoles-Dependent Activity Towards Surface Barrier of *Candida albicans*

Monika Staniszewska[a]*, Małgorzata Gizińska[a], Ewa Mikulak[a], Klaudia Adamus[b], Mirosława Koronkiewicz[c], Edyta Łukowska-Chojnacka[b]

[a]National Institute of Public Health-National Institute of Hygiene, Chocimska 24, 00-791 Warsaw, Poland

[b]Faculty of Chemistry, Warsaw University of Technology, Noakowskiego 3, 00-664 Warsaw, Poland

[c]National Medicines Institute, Warsaw, 00-725 Poland

*Correspondence: Monika Staniszewska, Independent Laboratory of Streptomyces and Fungi Imperfecti, National Institute of Public Health – National Institute of Hygiene, 24 Chocimska, 00-791 Warsaw, Poland

Phone: +48 22 54 21 228. Fax: + 48 22 849 74 84

E-mail: mstaniszewska@pzh.gov.pl

Abstract

A series of novel tetrazole derivatives was synthetized using *N*-alkylation or Michael-type addition reactions, and screened for their fungistatic potential against *Candida albicans* (the lack of endpoint = 100%). Among them, the selected compounds **2d**, **4b,** and **6a** differing in substituents at the tetrazole ring were non-toxic to *Galleria mellonella* larvae *in vivo* and exerted slight toxicity against Caco-2 *in vitro* (CC_{50} at 256 μg/mL). An antagonistic effect of tetrazole derivatives **2d**, **4b**, and **6a** respectively in combination with Fluconazole was shown using the checker board and colorimetric methods (fractional inhibitory concentration indexes FICIs >1). The most active **2d** and **6a** displayed an inverse relation between MICs in the presence of exogenous ergosterol, the effect was opposite to Itraconazole and Amphotericin B. The differences between **6a**'s and **2d**'s action mode were noted. Combining both flow cytometry and fluorescence image analyses respectively showed the complexity of planktonic and biofilm cell demise mode under the tetrazole derivatives tested. The following evidences for **6a**'s interaction with fungal membrane were noted: necrosis-like programmed cell death (97.03 ± 0.88), DNA denaturation (no laddering), mitochondrial damage (XTT assay), reduced adhesion to human epithelium (>50% at 0.0313 μg/mL, $p \leq 0.05$), irregular deposit of chitin, and attenuated morphogenesis in mature biofilm. The treatment with **6a** reduced pathogenicity of *C. albicans* during infection in *G. mellonella*. Contrariwise, **2d** enhancing fungal adhesion displayed mechanism targeted to the cell wall (due to the presence of 3-chloropropyl clubbed with aryltetrazole) in the presence of osmotic protector. Under **2d**, the accidental cell death (88.60% ± 4.81) was observed.

In conclusion, all tetrazole derivatives were obtained in satisfactory yields (60-95%) using efficient, simple and not expensive methods. Fungistatic and slightly anticancer tetrazole derivatives with the novel action mode can circumvent an appearance of antifungal-resistant strains. These results indicate that they are worthy of further studies.

Key words: *Candida albicans*; virulence; antifungal agents; tetrazole derivatives

Introduction:

Limited number of the available antifungal agents together with the emergence of resistant isolates created a need to search for novel antifungal compounds with a new mode of action and low cytotoxicity [1]. In this context, tetrazole derivatives represent a promising group of compounds displaying a wide range of biological activities, such as anticancer, anticonvulsant, anti-inflammatory, analgesic, antiproliferative, antibacterial, antifungal, antiparasitic and antiviral [2-5]. Tetrazole has poly-nitrogen electron-rich planar structural features, which allows tetrazole derivatives to easily bind with various enzymes or receptors *via* weak interactions, including hydrogen bounds, hydrophobic effect, coordination bonds or van der Waals force [4, 6]. Moreover, biological and physico-chemical properties of tetrazole derivatives can be modified by the attachment of several structurally distinct substituents to the heterocycle ring. This feature makes them desirable templates in many studies aimed at the development of new bioactive compounds [4]. Recently, new tetrazole-based antifungal drug candidates, VT-1129, VT-1161 and VT-1598, binding in the sterol 14α-demethylase's active site were described [5-9].

Recent evidences suggest that the majority of *Candida albicans* infections are associated with biofilm formation [7-9]. Once formed on central venous catheters (CVCs) or other implanted medical derives, fungal biofilm has the potential to seed disseminated bloodstream infections [10]. Approximately 8% of bloodstream infections originate in CVCs infected with *C. albicans* [11]. Moreover, fungal sessile cells display increased resistance to antifungal agents and host defence mechanisms, which may carry serious clinical consequences [7].

Recently there is a particular interest in developing non-mammalian *in vivo* models to study fungal virulence [12]. *Galleria mellonella* (greater wax moth) was introduced as an alternative host model to study microbial infections and for antimicrobial testing [12-15]. Herein, a series of novel tetrazole derivatives was synthesized and evaluated *in vitro* for activity against *C. albicans*. Afterwards, the three compounds: **2d**, **4b** and **6a** differing in substituents at the tetrazole ring were further assessed for cytotoxicity. More detailed mechanisms of anti-*C. albicans* action mode were elucidated in the case of the most effective inhibitors **6a** and **2d**. An effort was made to detect *C. albicans* cell death under these tetrazole derivatives. Following the trend in animal studies, we examined whether the novel tetrazole derivative **6a** reduces *C. albicans* virulence in the *G. mellonella* model *in vivo*.

Materials and Methods:

Fungal Strains, Media and Growth Conditions

The quality control *C. albicans* wild type strains: 90028 and SC5314 were purchased from American Type Culture Collection (ATCC). Reference strain was stored on ceramic beads in a Microbank tube (Prolab Diagnostics, Canada) at -70°C. Prior to the respective examinations, routine cultures were conducted at 30°C for 18 h in yeast extract–peptone–dextrose medium (YEPD) [16].

Synthesis of Tetrazole Derivatives

All the compounds were synthesized at the Faculty of Chemistry of the Warsaw University of Technology (Poland). In general, ^{1}H NMR (500 MHz) and ^{13}C NMR (125 MHz) spectra were recorded on Varian Mercury 500 MHz spectrometer (USA) in $CDCl_3$ solution; chemical shifts (δ) were reported in ppm. IR spectra were taken on a Carl Zeiss Specord M80 instrument (Germany). HRMS spectra were recorded on a Micro-mass ESI Q-ToF Premier instrument (Micromass UK Limited, Manchester UK). Melting points were determined in open capillaries and are uncorrected. The reactions were monitored by thin layer chromatography (TLC) aluminum plates with silica gel Kieselgel 60 F_{254} (thickness 0.2 mm, Merck, Germany) using UV light as visualizing agent. A column chromatography was performed using Kieselgel 60 (0.040–0.063 mm, Merck, Germany). Solvents and chemicals were purchased from POCH (Poland), Sigma-Aldrich (Germany) and Merck (Germany), and were used without further purification.

***N*-alkylation of 5-aryltetrazole 1a-d with 1-bromo-3-chloropropane**

To the solution of 5-aryltetrazole **1a-d** (3.47 mmol) in acetonitrile (20 mL), KOH (15 mmol, 0.84 g) dissolved in MeOH (7.5 mL), and 1-bromo-3-chloropropane (0.12 mol, 12 mL) were added. The mixture was stirred at reflux and the progress of the reaction was monitored by TLC using chloroform/methanol (100:1 v/v) as the eluent. After the appropriate time, the reaction was stopped and cooled to room temperature. Then, the inorganic solid was filtered off, and the residue evaporated under reduced pressure. Products were separated and purified on silica-gel column with hexane/ethyl acetate (50:1 v/v) as the eluent.

1-(3-chloropropyl)-5-phenyl-1*H*-tetrazole 2a. Yield 8%, oil. IR (film, cm^{-1}) 935, 996, 1021, 1037, 1075, 1108, 1120, 1149, 1181, 1405, 1536. ^{1}H NMR ($CDCl_3$) δ ppm: 2.42-2.47 (m, 2H, CH_2), 3.57-3.59 (m, 2H, CH_2Cl), 4.59-4.61 (m, 2H, CH_2N), 7.55-7.60 (m, 3H, Ar), 7.68-7.69 (m, 2H, Ar). ^{13}C NMR ($CDCl_3$) δ ppm: 31.97, 40.96, 45.10, 128.71, 128.85, 129.43, 131.37, 154.62. HRMS $[M+H]^+$ m/z calcd for $C_{10}H_{12}N_4Cl^+$ 223.0750 found 223.0643.

1-(3-chloropropyl)-5-(4-methylphenyl)-1*H*-tetrazole 2b. Yield 4%, oil. IR (film, cm^{-1}) 968, 1035, 1067, 1112, 1194, 1344, 1388, 1423, 1452, 1477, 1620. ^1H NMR ($CDCl_3$) δ ppm: 2.41-2.47 (m, 5H, CH_3, CH_2), 3.57-3.60 (m, 2H, CH_2Cl), 4.59 (t, 2H, CH_2N, J= 7.1 Hz), 7.35-7.38 (m, 2H, Ar), 7.57-7.60 (m, 2H, Ar). ^{13}C NMR ($CDCl_3$) δ ppm: 21.51, 31.96, 41.02, 45.10, 120.70, 126.73, 128.63, 129.58, 130.03, 141.86. HRMS $[M+H]^+$ m/z calcd for $C_{11}H_{15}N_4Cl^+$ 237.0907 found 237.0760.

5-(4-chlorophenyl)-1-(3-chloropropyl)-1*H*-tetrazole 2c. Yield 2%, oil. IR (film, cm^{-1}) 971, 1012, 1096, 1188, 1385, 1428, 1468, 1531, 1569, 1608. ^1H NMR ($CDCl_3$) δ ppm: 2.43-2.48 (m, 2H, CH_2), 3.57-3.59 (m, 2H, CH_2Cl), 4.57-4.60 (m, 2H, CH_2N), 7.54-7.56 (m, 2H, Ar), 7.64-7.66 (m, 2H, Ar). ^{13}C NMR ($CDCl_3$) δ ppm: 31.85, 40.93, 45.17, 122.11, 129.74, 130.08, 137.92, 153.77. HRMS $[M+H]^+$ m/z calcd for $C_{10}H_{11}N_4Cl_2^+$ 257.0361 found 257.0812.

5-(2-chlorophenyl)-1-(3-chloropropyl)-1*H*-tetrazole 2d. Yield 18%, oil. IR (film, cm^{-1}) 975, 1016, 1036, 1070, 1112, 1130, 1162, 1410, 1436, 1460, 1534, 1573, 1604. ^1H NMR ($CDCl_3$) δ ppm: 2.36-2.41 (m, 2H, CH_2), 3.49-3.52 (m, 2H, CH_2Cl), 4.41 (t, 2H, CH_2N, J=6.8 Hz), 7.46-7.60 (m, 4H, Ar). ^{13}C NMR ($CDCl_3$) δ ppm: 31.60, 40.83, 44.88, 123.59, 127.58, 130.35, 132.04, 132.73, 133.85, 152.96. HRMS $[M+H]^+$ m/z calcd for $C_{10}H_{11}N_4Cl_2^+$ 257.0361 found 257.0695.

2-(3-chloropropyl)-5-phenyl-2*H*-tetrazole 3a. Yield 52%, oil. IR (film, cm^{-1}) 924, 971, 1003, 1025, 1045, 1073, 1146, 1191, 1360, 1385, 1448, 1468, 1519, 1531. ^1H NMR ($CDCl_3$) δ ppm: 2.51-2.56 (m, 2H, CH_2), 3.63-3.65 (m, 2H, CH_2Cl), 4.84-4.86 (m, 2H, CH_2N), 7.45-7.51 (m, 3H, Ar), 8.13-8.17 (m, 2H, Ar). ^{13}C NMR ($CDCl_3$) δ ppm: 31.91, 41.00, 50.11, 126.82, 127.26, 128.89, 130.38, 165.29. HRMS $[M+H]^+$ m/z calcd for $C_{10}H_{12}N_4Cl^+$ 223.0750 found 223.0533.

2-(3-chloropropyl)-5-(4-methylphenyl)-2*H*-tetrazole 3b. Yield 58%, oil. IR (film, cm^{-1}) 971, 1044, 1178, 1194, 1366, 1420, 1464, 1512, 1544, 1560, 1624. ^1H NMR ($CDCl_3$) δ ppm: 2.41 (s, 3H, CH_3), 2.50-2.55 (m, 2H, CH_2), 3.62-3.65 (m, 2H, CH_2Cl), 4.82-4.85 (m, 2H, CH_2N), 7.30 (d, 2H, Ar, J = 8.3 Hz), 8.02-8.04 (m, 2H, Ar). ^{13}C NMR ($CDCl_3$) δ ppm: 21.48, 31.92, 41.02, 50.04, 124.46, 126.74, 129.58, 140.55, 165.38. HRMS $[M+H]^+$ m/z calcd for $C_{11}H_{15}N_4Cl^+$ 237.0907 found 237.0987.

5-(4-chlorophenyl)-2-(3-chloropropyl)-2*H*-tetrazole 3c. Yield 71%, colorless crystals mp 48-50°C. IR (nujol, cm^{-1}) 976, 1004, 1019, 1040, 1084, 1105, 1134, 1194, 1420, 1538, 1557,

1573, 1608. ^{1}H NMR ($CDCl_3$) δ ppm: 2.51-2.56 (m, 2H, CH_2), 3.62-3.65 (m, 2H, CH_2Cl), 4.84-4.87 (m, 2H, CH_2N), 7.45-7.48 (m, 2H, Ar), 8.07-8.09 (m, 2H, Ar). ^{13}C NMR ($CDCl_3$) δ ppm: 31.85, 40.95, 50.18, 125.75, 128.11, 129.20, 136.44, 164.43. HRMS $[M+H]^+$ m/z calcd for $C_{10}H_{11}N_4Cl_2^+$ 257.0361 found 257.0635.

5-(2-chlorophenyl)-2-(3-chloropropyl)-2*H*-tetrazole 3d. Yield 49%, oil. IR (film, cm^{-1}) 978, 1006, 1036, 1068, 1124, 1146, 1165, 1191, 1360, 1382, 1430, 1444, 1461, 1522, 1576, 1604. ^{1}H NMR ($CDCl_3$) δ ppm: 2.53-2.58 (m, 2H, CH_2), 3.65-3.67 (m, 2H, CH_2Cl), 4.89-4.92 (m, 2H, CH_2N), 7.37-7.43 (m, 2H, Ar), 7.53-7.55 (m, 1H, Ar). 7.941-7.960 (m, 1H, Ar). ^{13}C NMR ($CDCl_3$) δ ppm: 31.90, 40.98, 50.23, 126.38, 126.93, 130.84, 131.15, 131.32, 133.07, 163.47. HRMS $[M+H]^+$ m/z calcd for $C_{10}H_{11}N_4Cl_2^+$ 257.0361 found 257.0458.

Synthesis of tetrazole derivatives containing morpholine moiety 4a-d

To the solution of tetrazole **3a-d** (0.42 mmol) and morpholine (10.20 mmol, 0.9 mL) in acetonitrile (17 mL), K_2CO_3 (6.2 mmol, 0.857 g) was added. The reaction mixture was stirred at reflux and the progress of the reaction was monitored by TLC using chloroform/methanol (30:1 v/v) as the eluent. After 24 h a new portion of morpholine (10.20 mmol, 0.9 mL) was added. Finally, the reaction was stopped after 168 h, cooled to room temperature, and the inorganic solid was filtered off. The residue was concentrated under reduced pressure and purified on silica-gel column using chloroform/methanol (250:1 v/v) as the eluent.

4-[3-(5-phenyl-2*H*-tetrazol-2-yl)propyl]morpholine 4a. Yield 75%, oil. IR (film, cm^{-1}) 696, 732, 917, 959, 1006, 1028, 1045, 1072, 1116, 1143, 1200, 1360, 1382, 1448, 1461, 1528, 1620, 2812, 2858, 2899, 2960. ^{1}H NMR ($CDCl_3$) δ ppm: 2.20-2.25 (m, 2H, CH_2), 2.42-2.44 (m, 6H, CH_2N), 3.66-3,70 (m, 4H, CH_2O), 4.74 (t, 2H, CH_2tetr., J= 7.1 Hz), 7.45-7.50 (m, 3H, Ar), 8.12-8.15 (m, 2H, Ar). ^{13}C NMR ($CDCl_3$) δ ppm: 26.29, 51.31, 53.56, 55.25, 66.93, 126.75, 127.47, 128.87, 130.24. HRMS $[M+H]^+$ m/z calcd for $C_{14}H_{20}N_5O^+$ 274.1162 found 274.1162.

4-{3-[5-(4-methylphenyl)-2*H*-tetrazol-2-yl]propyl}morpholine 4b. Yield 83%, colorless crystals mp 38–40°C. IR (nujol, cm^{-1}) 685, 756, 916, 955, 1010, 1029, 1044, 1072, 1120, 1143, 1185, 1360, 1375, 1417, 1452, 1464, 1544, 1620, 2817, 2856, 2956. ^{1}H NMR ($CDCl_3$) δ ppm: 2.19-2.24 (m, 2H, CH_2), 2.41-2.44 (m, 9H, CH_3, CH_2N), 3.67-3.68 (m, 4H, CH_2O), 4.73 (t, 2H, CH_2tetr., J=6.8 Hz), 7.28-7.30 (m, 2H, Ar), 8.00-8.03 (m, 2H, Ar). ^{13}C NMR

($CDCl_3$) δ ppm: 21.53, 26.30, 51.26, 53.57, 55.27, 66.94, 124.68, 126.66, 129.47, 129.65, 140.37, 165.37. HRMS $[M+H]^+$ m/z calcd for $C_{15}H_{23}N_5O^+$ 288.1819 found 288,1919.

4-{3-[5-(4-chlorophenyl)-2*H*-tetrazol-2-yl]propyl}morpholine 4c. Yield 77%, colorless crystals mp 73-75°C. IR (nujol, cm-1) 695, 756, 920, 972, 1016, 1048, 1076, 1092, 1116, 1153, 1181, 1200, 1337, 1364, 1420, 1448, 1464, 1522, 1582, 1608, 2816, 2867, 2944. ^{1}H NMR ($CDCl_3$) δ ppm: 2.19-2.24 (m, 2H, CH_2), 2.41-2.44 (m, 6H, CH_2N), 3.66-3.69 (m, 4H, CH_2O), 4.74 (m, 2H, CH_2tetr., J= 7.1 Hz), 7.45-7.47 (m, 2H, Ar), 8.06-8.09 (m, 2H, Ar). ^{13}C NMR ($CDCl_3$) δ ppm: 26.27, 51.40, 53.56, 55.23, 66.93, 125.98, 128.03, 129.08, 129.26, 136.27, 164.17. HRMS $[M+H]^+$ m/z calcd for $C_{14}H_{19}N_5OCl^+$ 308.1272 found 308.8911.

4-{3-[5-(2-chlorophenyl)-2*H*-tetrazol-2-yl]propyl}morpholine 4d. Yield 87%, oil. IR (film, cm^{-1}) 752, 778, 916, 954, 1012, 1036, 1068, 1120, 1146, 1356, 1385, 1440, 1460, 1520, 1574, 1604, 2811, 2856, 2888, 2956. ^{1}H NMR ($CDCl_3$) δ ppm: 2.21-2.27 (m, 2H, CH_2), 2.43-2.46 (m, 6H, CH_2N), 3.66-3.69 (m, 4H, CH_2O), 4.77-4.80 (m, 2H, CH_2tetr.), 7.36-7.42 (m, 2H, Ar), 7.52-7.54 (m, 1H, Ar), 7.94-7.95 (m, 1H, Ar). ^{13}C NMR ($CDCl_3$) δ ppm: 26.28, 51.44, 53.56, 55.24, 66.94, 126.58, 126.91, 130.82, 131.03, 131.29, 133.00, 163.21. HRMS $[M+H]^+$ m/z calcd for $C_{14}H_{19}N_5OCl^+$ 308.1272 found 308.8911.

Michael-type addition of ethyl acrylate to 5-aryltetrazole 1a-d

To the solution of 5-arylterazole **1a-d** (3.2 mmol) in 2-propanol (10 mL) ethyl acrylate (4.65 mmol, 0.5 mL) and Et_3N (2.87 mmol, 0.4 mL) were added. The reaction mixture was stirred at reflux and the progress of the reaction was controlled by TLC using chloroform/methanol (100:1 v/v) as the eluent. After the appropriate time, the reaction was stopped. The solvent and the excess of Et_3N were evaporated under reduced pressure, and products were separated and purified on silica-gel column using chloroform/methanol (1200:1 v/v) as the eluent.

ethyl 3-(5-phenyl-1*H*-tetrazol-1-yl)propanoate 5a. Yield 9%, oil. IR (film, cm^{-1}) 940, 1029, 1076, 1111, 1200, 1350, 1382, 1404, 1468, 1534, 1608, 1736. ^{1}H NMR ($CDCl_3$) δ ppm: 1.21 (t, 3H, CH_3, J = 7.3 Hz), 3.07 (t, 2H, CH_2CO, J=6.8 Hz), 4.11 (q, 2H, OCH_2CH_3, J= 7.3 Hz), 4.64-4.67 (m, 2H, CH_2N), 7.56-7.59 (m, 3H, Ar), 7.71-7.73 (m, 2H, Ar). ^{13}C NMR ($CDCl_3$) δ ppm: 14.02, 33.57, 43.53, 61.33, 123.81, 128.87, 129.29, 131.31, 154.61, 169.71. HRMS $[M+H]^+$ m/z calcd for $C_{12}H_{15}N_4O_2^+$ 247.1195 found 247.1390.

ethyl 3-[5-(4-methylphenyl)-1*H*-tetrazol-1-yl]propanoate 5b. Yield 10%, oil. IR (film, cm^{-1}) 946, 1024, 1108, 1196, 1372, 1417, 1452, 1464, 1480, 1620, 1732. ^{1}H NMR ($CDCl_3$) δ

ppm: 1.21 (t, 3H, CH_3, *J* = 7.1 Hz), 2.45 (s, 3H, CH_3Ar), 3.06 (t, 2H, CH_2CO, *J*= 6.8 Hz), 4.11 (q, 2H, OCH_2CH_3, *J* = 7.1 Hz), 4.64-4.67 (m, 2H, CH_2N), 7.36-7.38 (m, 2H, Ar), 7.60-7.62 (m, 2H, Ar). ^{13}C NMR ($CDCl_3$) δ ppm: 14.03, 21.51, 33.61, 43.49, 61.31, 120.81, 128.71, 129.99, 141.77, 154.63, 169.71. HRMS $[M+H]^+$ m/z calcd for $C_{13}H_{17}N_4O_2^+$ 261.1352 found 261.1302.

ethyl 3-[5-(2-chlorophenyl)-1*H*-tetrazol-1-yl]propanoate 5d. Yield 28%, oil. IR (film, cm^{-1}) 948, 1036, 1075, 1112, 1130, 1196, 1350, 1379, 1408, 1440, 1460, 1532, 1571, 1604, 1736. ^1H NMR ($CDCl_3$) δ ppm: 1.21 (t, 3H, CH_3, *J* = 7.3 Hz), 3.02 (t, 2H, CH_2CO, *J*= 6.8 Hz), 4.09 (q, 2H, OCH_2CH_3, *J* = 7.3 Hz), 4.47 (t, 2H, CH_2N, *J*= 6.8 Hz), 7.45-7.58 (m, 4H, Ar). ^{13}C NMR ($CDCl_3$) δ ppm: 13.99, 33.35, 43.35, 61.26, 123.71, 127.53, 130.21, 132.13, 132.68, 133.82, 152.93, 169.61. HRMS $[M+H]^+$ m/z calcd for $C_{12}H_{14}N_4O_2Cl^+$ 281.0805 found 281.1228.

ethyl 3-(5-phenyl-2*H*-tetrazol-2-yl)propanoate 6a. Yield 86%, oil. IR (film, cm^{-1}) 924, 946, 1028, 1041, 1073, 1192, 1360, 1372, 1404, 1452, 1464, 1534, 1736. ^1H NMR ($CDCl_3$) δ ppm: 1.26 (t, 3H, CH_3, *J* = 7.3 Hz), 3.11-3.13 (m, 2H, CH_2CO), 4.19 (q, 2H, OCH_2CH_3, *J*=7.3 Hz), 4.93-4.96 (m, 2H, CH_2N), 7.46-7.50 (m, 3H, Ar), 8.12-8.14 (m, 2H, Ar). ^{13}C NMR ($CDCl_3$) δ ppm: 14.10, 33.58, 48.53, 61.27, 126.81, 127.30, 128.86, 130.32, 165.19, 169.62. HRMS $[M+H]^+$ m/z calcd for $C_{12}H_{15}N_4O_2^+$ 247.1195 found 247.1148.

ethyl 3-[5-(4-methylphenyl)-2*H*-tetrazol-2-yl]propanoate 6b. Yield 80% solidifying oil. IR (nujol, cm^{-1}) 936, 1024, 1045, 1070, 1115, 1192, 1407, 1449, 1538, 1560, 1617, 1744. ^1H NMR ($CDCl_3$) δ ppm: 1.26 (t, 3H, CH_3, *J* = 7.3 Hz), 2.41 (s, 3H, CH_3Ar), 3.10-3.13 (m, 2H, CH_2CO), 4.19 (q, 2H, OCH_2CH_3, *J* = 7.3 Hz), 4.92-4.95 (m, 2H, CH_2N), 7.28-7.29 (m, 2H, Ar), 8.01-8.02 (m, 2H, Ar). ^{13}C NMR ($CDCl_3$) δ ppm: 14.10, 21.47, 33.60, 48.47, 61.26, 124.50, 126.73, 129.55, 140.48, 165.27, 169.65. HRMS $[M+H]^+$ m/z calcd for $C_{13}H_{17}N_4O_2^+$ 261.1352 found 261.1302.

ethyl 3-[5-(4-chlorophenyl)-2*H*-tetrazol-2-yl]propanoate 6c. Yield 85%, colorless crystals mp 49-50°C. IR (nujol, cm^{-1}) 1004, 1016, 1041, 1092, 1172, 1404, 1420, 1608, 1736. ^1H NMR ($CDCl_3$) δ ppm: 1.26 (t, 3H, CH_3, *J* = 7.3 Hz), 3.12 (t, 2H, CH_2CO, *J*= 6.8 Hz), 4.19 (q, 2H, OCH_2CH_3, *J*= 7.3 Hz), 4.93-4.96 (m, 2H, CH_2N), 7.44-7.47 (m, 2H, Ar), 8.05-8.08 (m, 2H, Ar). ^{13}C NMR ($CDCl_3$) δ ppm: 14.15, 33.51, 48.60, 61.32, 125.79, 128.10, 129.09, 129.25, 136.38, 164.31, 169.57. HRMS $[M+H]^+$ m/z calcd for $C_{12}H_{14}N_4O_2Cl^+$ 281.0805 found 281.0549.

ethyl 3-[5-(2-chlorophenyl)-2*H*-tetrazol-2-yl]propanoate 6d. Yield 47%, oil. IR (film, cm^{-1}) 946, 1036, 1064, 1095, 1127, 1192, 1350, 1375, 1398, 1423, 1444, 1461, 1519, 1576, 1601, 1736. ^{1}H NMR ($CDCl_3$) δ ppm: 1.25 (t, 3H, CH_3, J = 7.1 Hz), 3.14 (t, 2H, CH_2CO, J=7.1 Hz), 4.19 (q, 2H, OCH_2CH_3, J = 7.1 Hz), 4.98-5.01 (m, 2H, CH_2N), 7.36-7.24 (m, 2H, Ar), 7.52-7.54 (m, 1H, Ar), 7.93-7.95 (m, 1H, Ar). ^{13}C NMR ($CDCl_3$) δ ppm: 14.09, 33.54, 48.66, 61.29, 126.40, 126.89, 130.83, 131.09, 131.31, 133.05, 163.37, 169.58. HRMS $[M+H]^+$ m/z calcd for $C_{12}H_{14}N_4O_2Cl^+$ 281.0805 found 281.0425.

Antifungal Activity Assay against *C. albicans*

A susceptibility of planktonic cells of *C. albicans* reference strain 90028 to novel tetrazole derivatives was determined using M27-A3 method [17]. The final inoculum of $1.8x10^3$ cells/mL was prepared in the synthetic RPMI 1640 medium at pH 7.0 buffered with morpholinepropanesulfonic acid (MOPS). Compounds' concentrations ranging from 0.0313 to 16 µg/mL were prepared with stock solution of compounds (1600 µg/mL) dissolved either in 40% ethanol (**3c**, **4c**, **6c-d**), or 50% (**6a-b**, **5a-b**, **5d**, **3a**, **2a**, **2d**, **4a-b, 4d**) and 70% DMSO (**3b**, **3d**). Amphotericin B (Sigma–Aldrich, USA) was diluted in DMSO (1600 µg/mL) to be subsequently used in the assay as a reference antifungal at the concentration of 0.5 µg/mL (100% cell inhibition – clear endpoint). Microtiter plates were incubated at 35°C without agitation for 48 h. After incubation, the growth of cells was measured by microtiter plate reader Spark Control M10 (Tecan Group Ltd., Austria). Minimal inhibitory concentration (MIC) was defined as the lowest concentration of the compounds that yielded no visible growth. The endpoint was calculated as a 100% reduction in OD_{405} as compared to the growth in control wells. Percentage of the cell growth inhibition was calculated according to the following formula: % of inhibition = 100 - (OD_{405} CTW - OD_{405} SCW)/(OD_{405} GCW - OD_{405} SCW) [18]. CTW were prepared with compound, medium and inoculum; SCW wells contained compound, RPMI 1640 medium and sterile water replacing inoculum; GCW were prepared with inoculum, RPMI 1640 medium and the same amount of DMSO/ethanol used in CTW.

The minimal fungicidal concentration (MFC) was determined as described previously [16, 19-20]. Briefly, 50 µL aliquots from the selected wells of plates were removed after 48 h of incubation at 35°C. Next, after 1/10,000 dilutions, 100 µL aliquots were placed onto agent-free Sabouraud dextrose agar plates and incubated at 35ºC for 48 h. The MFC results for each tetrazole concentration tested were defined as the reduction viability record (R) and calculated using the formula: R = lg CFU/mL control cells – lg CFU/mL tetrazole treated cells. The

lowest tetrazole concentration demonstrating a minimum 10^3 reduction in viable count ($\lg R \geq 3$) was defined as MFC [16, 19-20].

Cytotoxicity Assay

To test the *in vitro* cytotoxicity, the lead fungistatic compounds: **2d**, **4b**, and **6a** derived from different chemical syntheses were screened. In order to discriminate three cytotoxicity potency values (increasing, optimal, and decreasing) the following concentrations were tested: 256, 16 and 0.0313 μg/mL. Briefly, cytotoxicity against Caco-2 cells (ATCC HTB-37, LGC, Poland) using 2,3-bis(2-methoxy-4-nitro-5-sulfophenyl)-2*H*-tetrazolium-5-carboxanilide (XTT, Roche Diagnostics GmbH, Mannheim, Germany) was evaluated as described in [21]. Each well was treated with 50 μL of XTT reagent for 4-6 h. The concentration at which the cell viability had dropped by 50% was recorded as the cytotoxic concentration (CC_{50}) [22]. The optical densities at 475 nm (660 nm reference wavelength) were measured using a plate reader Spark Control M10 (Tecan Group Ltd., Austria).

Additionally, based on the *in vitro* cytotoxicity data, the leading agents: **2d** and **6a**, displaying the best cytotoxic efficiency against Caco-2, were tested in the *G. mellonella*-based model *in vivo*. The larvae were injected with the RPMI-obtained compounds' concentrations of 256, 16 and 0.0313 μg/mL, with the mixture free of the *Candida* suspension, as described previously [23]. A group of 10 larvae were injected with the above compounds' concentrations in parallel. Then, the larvae were placed in 9.2 cm Petri dishes, kept at 37°C in darkness up to 96 h, and monitored daily. As larvae's response to the RPMI injection is comparable with the PBS one (both non-toxic) [24], in the experiment we included only PBS. Thus, the PBS-inoculated larvae were used as the controls, to ensure that the death was not due to injection trauma. Insects were considered dead when they did not respond to physical stimuli [22]. Additionally, the larvae health status was evaluated by assessing larvae mobility, cocoon formation, melanization and survival. The each attribute contributing to an overall health of an individual larva was scored and health index was calculated as described previously [14]. No significant difference in the larval survival between the tetrazole-treated larvae and control group would indicate that the tested agent is not toxic at the examined doses [25].

Assessment of the Fractional Inhibitory Concentration (FIC)

To determine the respective interactions of compounds **2d**, **4b,** or **6a** with Fluconazole (Flc), the microdilution assays were carried out following the method M27-A3 [17] in the following endpoint criterion [20]: total inhibition – the compound concentration yielding 100% growth

inhibition. Fluconazole (Sigma–Aldrich, USA) stock solution (5120 μg/mL) was prepared with water and subsequently final concentrations were diluted with the RPMI medium.

Fluconazole was tested against *C. albicans* according to the method M27-A3 [17]. The fractional inhibitory concentration (FIC) of each compound tested and their total FIC indexes were determined by using a checkerboard assay [23, 26]. Briefly, the checkboards were prepared by using serial dilutions of Flc (80-1.25 μg/mL) in the horizontal wells and compounds: **2d**, **4b**, or **6a** respectively at the final concentrations from 80 to 1.25 μg/mL in the vertical wells. Yeast suspension was prepared according to the method M27-A3 [17] and 100 μL was inoculated into the each well of a 96-well microtiter plate. The microplates were incubated at 35°C for 48 h. The growth rate of *C. albicans* ATCC 90028 was assessed spectrophotometrically at 405 nm (Spark Control M10, Tecan Group Ltd., Austria) after 18 and 48 h. Additionally, the combined activity of tetrazoles: **2d**, **4b**, or **6a** respectively with Flc against *C. albicans'* metabolic activity was determined after 48 h using the metabolic reduction assay (XTT, Roche Diagnostics GmbH, Mannheim, Germany), with reading at 475 nm (660 nm reference wavelength). The antifungal effect was measured by comparing the reduction in the mean absorbance of the compound-treated well to that of untreated growth control [27]. In order to characterize the interaction of each combination tested, the fractional inhibitory concentrations (FICs) of each agent tested and their sums are used to calculate the FIC index for the cells' metabolic reduction and endpoint (100% growth reduction). As defined, the FIC index of <1 is the expression of the agents' synergism, whereas the FIC index of >1 represents an antagonism [23, 28].

Adhesion Assay

As the loss of adherence is demonstrated by the necrotic treatment we assessed the cell adhesion inhibition under **2d**, **4b**, and **6a** to Caco-2 monolayer as described in [22, 29]. For the experiment, Caco-2 cells were seeded at the density of $1.2x10^5$ cells/mL into 24-well-plates (Corning, USA) and cultured in the EMEM medium (10 vol. % FCS, 1 mM pyruvic acid; ATCC, USA) without antibiotics or antifungal agents for 18 h [29].

Yeast cells were grown for 18 h in YEPD at 30°C, and then pre-treated with **2d**, **4b**, and **6a**, respectively. Two hundred microliters of blastoconidial suspension (at final density of 10^4/mL) were pre-incubated with 1,800 μL of the RPMI medium (containing selected concentration of the compound) for 2 h on a shaker at 35°C. Then, cells were washed twice with phosphate-buffered saline (PBS) and re-suspended in 2,000 μL of fresh RPMI medium. The adherent endothelial Caco-2 cells were washed twice with PBS before incubation with

blastoconidial suspension (pre-treated with compound) for 2 h at 37°C in a humidified atmosphere with 5% CO_2 (vol/vol). Afterwards, the non-adherent cells were removed by standard rinsing. The Caco-2 cell line was lysed by adding sterile water resulting with *C. albicans* cells' recovery. After 18-h growth on the Sabouraud dextrose agar plates at 30°C, the number of adherent cells was determined by colony counting and compared with the controls. The adhesion of the untreated cells was assessed as described above (but without antifungal compound). Adherence was expressed as a percentage of the total number of cells added (control cells) [22, 29].

Test with Sorbitol

Since both **2d** and **6a** were the leading tetrazole derivatives with the anticancer efficiency and reduced toxicity, their MICs in the presence of an osmotic protector were determined using the method M27-A3 [17] and previously described protocols [16, 30]. Sabouraud dextrose broth (SDB) medium was added to the each well of the microplate and the serial dilutions of tetrazole derivatives (1.04–400 μg/mL) were carried. Afterwards, 100 μL of *C. albicans* inoculum ($1.7x10^3$ CFU/mL) prepared in Sabouraud dextrose broth medium supplemented with sorbitol at final concentration of 0.8 M (Sigma-Aldrich, USA) was transferred to wells as described previously [16, 30]. Plates were incubated at 35°C and then read visually and spectrophotometrically at 405 nm (Spark Control M10, Tecan Group Ltd., Austria) after 2 and 7 days.

***C. albicans* Biofilm Cell-Death Assessment with Nuclear Staining Techniques under Confocal Laser Scanning Microscope**

Since **6a** reduced significantly (at $p \leq 0.05$) the adherence of *C. albicans* (initial step of biofilm formation) to Caco-2, the compound was then used to assess the mature biofilm cell-death. TR146 cells were cultured in D-MEM with 10% of fetal bovine serum (FBS) and 0.1% of gentamicin solution (50 mg/mL) at 37°C and 5% of CO_2. For the experiment, TR146 cells were seeded at the density of $1.2x10^5$ cells/mL into 12-well-plates with polycarbonate filter inserts (Corning, USA). To assess the influence of **6a** on the *C. albicans* biofilm formation, the TR146 cell line after 21-day post seeding was inoculated with $1.0\text{-}1.2x10^5$/mL of the log-phase yeast cells of 90028 ATCC. Afterwards, the biofilms were pre-treated with **6a** at 256, 16, or 0.0313 μg/mL separately for 18-48 h (37°C in 5 vol % CO_2). After double washing with PBS, we separately used three staining methods that provided the illustration of cells' abnormality and their content in fluorescence microscopy. Accordingly, propidium iodide (PI, 5 μg/mL, Roche Diagnostics GmbH, Mannheim, Germany) was used as a marker for degenerating cells (without fixation). Acridine orange (Sigma, USA) staining was elaborated

to show DNA denaturation *in situ* in the apoptotic cells under the tested tetrazole derivatives. Additionally, the cells treated with tetrazole derivatives were stained with Calcofluor white (10 mg/mL, Sigma Aldrich, USA) to depict chitin content according to the manufacturer's instruction. The influence of **6a** on the *C. albicans* biofilm generated on TR146 was assessed using the Olympus FLUOROVIEW FV1000 confocal laser scanning microscope CLSM (Olympus, USA). Images were assembled using the Photoshop software (Adobe Photoshop CS3 Extended, France).

Additionally, a Comet assay was used to detect DNA damage in the **6a**-pretreated cells and suspended in 1% melted agarose gel, cast on microscope slides and immersed in alkaline detergent (2.5 M NaCL, 100 mM Na_2EDTA, Tris-HCL, 1% Na-sarcosinate, pH 10) following gelling in order to lyse cells. The experiment was prepared according to the protocol described by Olive and Banáth [31] subsequently including: low-gelling-temperature agarose, slide precoating, **6a-**treated and untreated samples, and alkaline lysis followed by electrophoresis (5 V/cm for 5 min) under alkaline conditions, consecutively by DNA staining with fluorescent ethidium bromide generating red emission signals under the fluorescence microscope CLSM (Olympus, USA). This method was confirmed by the detection of apoptosis in the **6a**-treated cells with the technique that involves the extraction of nuclear DNA and assessment of the oligonucleosomal ladder with gel electrophoresis [32-33]. Briefly, the extracted DNA from the **6a**-treated and untreated cells was loaded on 1.5% agarose gel containing 1.4 μg/mL ethidium bromide. Additionally, DNA denaturated at 100°C for 10 min was included as a negative control. The gel was examined and photographed by the ultraviolet gel documentation system (iNTAS, Goettingen, Germany).

Flow Cytometry Analysis

Additionally, flow cytometry technique was adapted for the aborted apoptosis measurement. Generation and labelling of *Candida* protoplasts with the Annexin-V-FLUOS method was performed as described in [34]. In compliance with the statement of the cell wall impermeability for Annexin-V and our prediction that tetrazoles **2d** and **6a** interact with the plasma membrane, we generated protoplasts followed by their sensitivity to 5% SDS lysis as described previously [34]. After the pre-treatment of the protoplasts with **6a** or **2d,** they were stained with Fluorescein-labelled (FITC) annexin-V and propidium iodide (PI) using the Annexin-V-FLUOS Staining Kit (Roche Diagnostics GmbH, Mannheim, Germany). The annexin-V and (PI) status of a minimum of 5,000 protoplasts was recorded for each treatment and the measurement was repeated in three independent experiments. Flow cytometry

analyses were run on a FACSCanto II flow cytometer (BD Biosciences, San Jose CA, USA), and analyzed using the BD FACSDiva software.

Efficacy of 6a in *G. mellonella* Infected with *C. albicans*

Since solely **6a** was active against the initial and mature biofilm formation, appearing in the mucosal candidiasis *in vivo* [24], this agent was used in further studies, as described below. The compound was tested in the lowest most effective anti-biofilm concentration, namely 16 μg/mL. The later concentration was obtained by dilution of the stock conc. of 1600 μg/mL in the RPMI medium. Larvae were accordingly selected by weight (195±17 mg) and disinfected using ethanol 70% (vol/vol). The larvae killing assays were performed as described in [22]. Briefly, the larvae were injected with 10 μL of *C. albicans* suspension into the last right proleg using a Hamilton syringe. Afterwards, larvae were injected with 10 μL of single treatment dose of **6a** (at 16 μg/mL RPMI) into last left proleg after 30 min or 1 h, respectively. To assess the ability of **6a** to protect larvae against subsequent *C. albicans* infection, single treatment doses of the compound were given 1 h or 30 min prior inoculation. The larvae injected with *C. albicans* or PBS instead of **6a** were used as the positive or negative control respectively. The larvae survival was monitored every 24 h for 2 days. The health index was calculated as described previously [14]. At least three independent experiments were performed; with experimental values expressed as means±standard error of the mean (SEM) [14].

Test with Ergosterol

6a's and **2d**'s interaction with exogenous ergosterol (Sigma-Aldrich, St. Louis, MO, USA) was determined using the method M27-A3 [17] with a few modifications. The following four compounds were tested: **6a**, **2d**, Itraconazole (ITR), and Amphotericin B (AmB), respectively at the range of concentrations from 512 to 1 μg/mL (tetrazole and ITR) and from 125 to 0.24 μg/mL (AmB). Briefly, the amount of 200 μL of the tested compound at the concentration of 1.024 μg/mL or 250 μg/mL was put into the first column of the microtiter plate. Simultaneously, RPMI (100 μL) was added to the tested wells except for the wells of the first column. Then, the compound was serially diluted and subsequently it was removed (100 μL) from the tenth well. The final inoculum of yeast suspension recommended by M27-A3 (10^3 CFU/mL) was prepared in RPMI supplemented with ergosterol and distributed to the wells in the volume of 100 μL, giving ergosterol's final concentration of 400 μg/mL in the tested wells. The ergosterol had been prepared directly before the experiment. It was dissolved in 10% DMSO (v/v), and 1% Tween 80 (v/v), heated to augment the solubility, and then diluted

with the RPMI medium. ITR and AmB were tested as positive controls, and yeast growth and sterility were also controlled. The plates were incubated at 35°C and then read after 72 h. This assay was carried out in triplicate and then repeated on three different days. The geometric mean values were calculated for each experiment. MIC was determined as the lowest concentration of the compound which inhibited the visible fungal growth.

Statistical Analysis

Each experiment was performed at least three times on three different occasions; with the experimental values expressed as means±SD. Statistical differences between the control and test values were determined by means of the Wilcoxon signed-rank matched-pair test. The p values ≤ 0.05 were considered to be statistically significant.

Results

Chemistry

A chemical synthesis involved preparation of tetrazole derivatives including 1-(3-chloropropyl)-5-aryltetrazoles **2a-d** and **3a-d**, tetrazole derivatives containing morpholine moiety **4a-d** and propionate esters substituted by various 5-arylterazole **5a-d** and **6a-d**. 5-Aryltetrazole **1a-d** required for these syntheses were prepared according to the described method [35]. Compounds **2a-d** and **3a-d** were obtained by *N*-alkylation of appropriate 5-aryletrazole **1a-d** with 1-bromo-3-chloropropane (Fig. 1). The reaction was carried out in the presence of KOH in solution of acetonitrile and MeOH at reflux. The progress of the reaction was monitored by thin-layer chromatography.

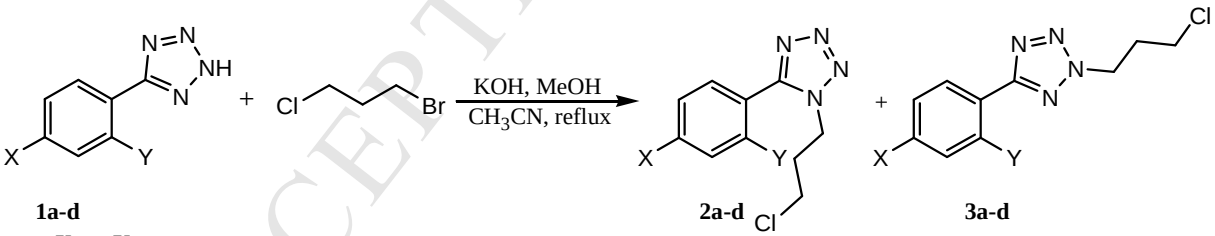

	X	Y
a -	H	H
b -	CH_3	H
c -	Cl	H
d -	H	Cl

Fig. 1. *N*-alkylation of 5-aryltetrazole **1a-d**

In all cases the formation of two isomers, 1,5- and 2,5-disubstituted tetrazoles, was observed. The reaction was highly regioselective and preferential alkylation at the 2-position of tetrazole ring took place (Table 1). The weight ratio of isomers **2a-d** to **3a-d** depended on the aryl substituent at 5-position of tetrazole ring. The highest regioselectivity (isomers ratio 50:1) was observed for *N*-alkylation of 5-(4-chlorophenyl)-1*H*-tetrazole **1c**, whereas the lowest for *N*-

alkylation of 5-(2-chlorophenyl)-1*H*-tetrazole **1d** (isomers ratio 3:1). Furthermore, depending on the aryl substituent at tetrazole ring the reaction took place in various time ranging from 3.5 to 5.5 h indicating the dependency of the reaction rate from steric congestion (Table 1).

Table 1 Reaction time, total yields and isomers ratios of tetrazole derivatives **2a-d** to **3a-d**

Compound	X	Y	Time (h)	Yield (%)	Isomers ratio (2:3)
2a + **3a**	H	H	3.5	60	7:1
2b + **3b**	CH_3	H	3.5	62	15:1
2c + **3c**	Cl	H	4.5	67	50:1
2d + **3d**	H	Cl	5.5	73	3:1

Isomers **2a-d** and **3a-d** were separated and purified on a column chromatography on silica gel and obtained with satisfactory total yields of 60-73%. It is worth pointing out that the regioselective alkylation of tetrazoles was previously mentioned in the work concerning synthesis of compound **3a** (authors did not state the isomers ratio) [36], and in other works [37-38].

In order to obtain more complex molecules and study the structure-activity relationships chlorine atom in tetrazole derivative **3a-d** was replaced by morpholine moiety. Thus disubstituted tetrazole derivatives **3a-d** were used as alkylating agents in *N*-alkylation of morpholine (Fig. 2). The reaction was performed in the presence of K_2CO_3, in acetonitrile at reflux. The progress of the reaction was monitored on TLC plates using chloroform/methanol as the eluent.

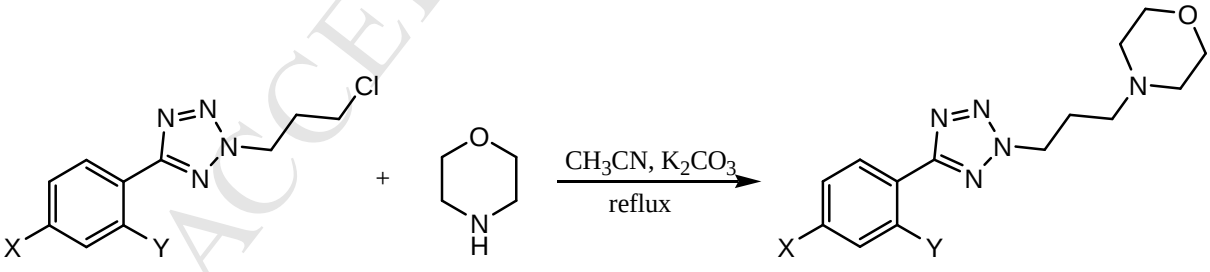

3a-d **4a-d**

Fig. 2. Synthesis of tetrazole derivatives bearing morpholine moiety **4a-d**

Regardless of the substrate the 100% conversion was reached after 168 h. All products were purified on a column chromatography on silica gel and obtained with high yields ranging from 75 to 87% (Table 2).

Table 2 Reaction time and yields of synthesis of tetrazole derivatives containing morpholine moiety **4a-d**

Compound	X	Y	Time (h)	Yield (%)
4a	H	H	168	75
4b	CH_3	H		83
6c	Cl	H		77
4d	H	Cl		87

The third group of synthesized tetrazole derivatives were propionate esters **5a-d** and **6a-d**. These compounds were obtained by Michael-type addition of 5-aryltetrazole **1a-d** to ethyl acrylate (Fig. 3). The reaction was carried out in 2-propanol, in the presence at Et_3N at reflux. The progress of the reaction was controlled using TLC plates.

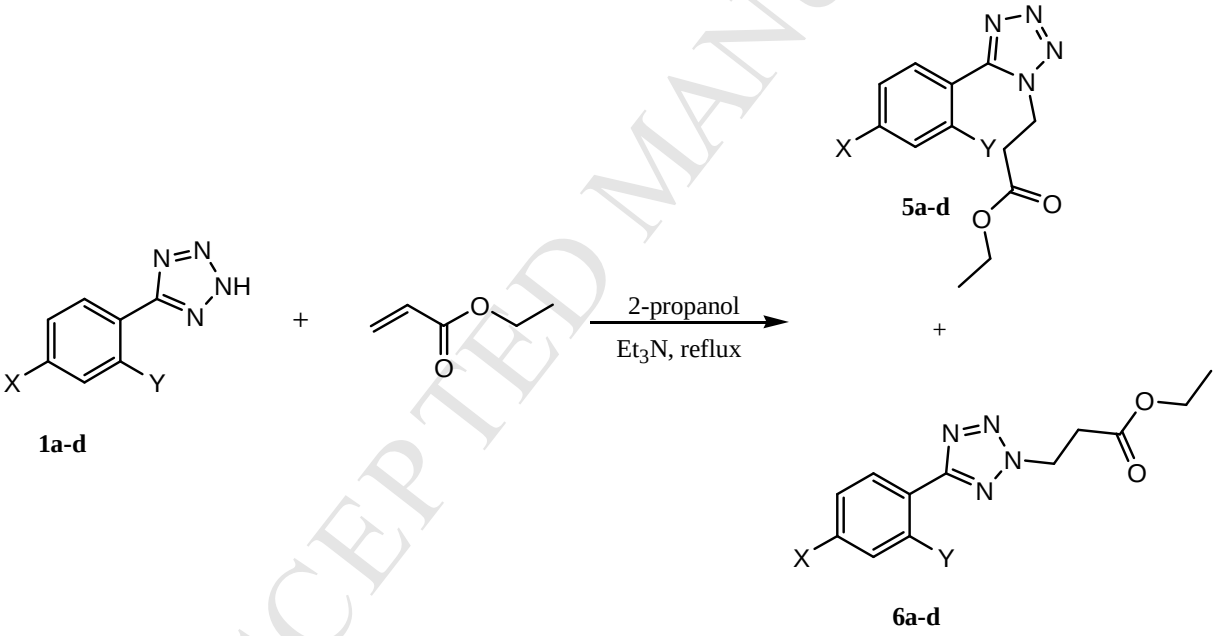

Fig. 3. Michael-type addition of 5-aryltetrazole **1a-d** to ethyl acrylate

As in the case of *N*-alkylation of 5-arylterazole **1a-d** with 1-bromo-3-chloropropan, these reactions also took place regioselectively and formation of 2,5-disubstituted tetrazole **6a-d** was preferred, but not exclusive. The weight isomers ratios were summarized in Table 3.

Table 3 Reaction time, total yields and isomers ratio of tetrazole derivatives **5a-d** to **6a-d**

Compounds	X	Y	Time (h)	Yield (%)	Isomers ratio (5:6)
5a + **6a**	H	H	168	95	9.2:1
5b + **6b**	CH_3	H	168	90	8.6.1
6c	Cl	H	162.5	85	1:0
5d + **6d**	H	Cl	162.5	75	2.6:1

1,5-Disubtiuted tetrazoles, were separated and purified in three cases (**5a**, **5b**, **5d**). Isomer **5c** was formed in trace amounts, which was sufficient only for HRMS analysis, therefore the isomers ratio was calculated as 1:0.

Biological Evaluation

Terazole Derivatives as Inhibitors of *C. albicans* Growth without Fungicidal Properties

The antifungal screening revealed that all the synthesized tetrazole derivatives were active against *C. albicans*, demonstrating the moderate-to-good cell growth inhibition at 0.0313-16 μg/mL (Table 4). Additionally, four compounds (**3c**, **4c,** and **6c-d**) fully inhibited the growth of *C. albicans* (100% cell reduction) at 16 μg/mL after 18 h. This showed small structure-activity relationships, the four compounds are 2,5-disubstituted tetrazoles and all contain chlorine substituent at the benzene ring. The substituent types at *N-1* or *N-2* of the tetrazole ring exhibited little antifungal effect of the synthesized derivatives. Neither clear endpoint nor fungicidal activity (R≥3 lg) (Table 5) were observed after 48-h incubation of the reference *C. albicans* cells with the tested compounds in the microdilution method M27-A3. No visual MIC was observed either after 18 or 48 h of the yeast cells incubation with each tetrazole derivative.

Table 4 Antifungal Activity (Cells Inhibition %; Means±SD) of Tetrazole Derivatives Against the Reference *C. albicans* Strain ATCC 90028

Compound	Incubation time (h)	Concentration (μg/mL)[a]									
		16	**8**	**4**	**2**	**1**	**0.5**	**0.25**	**0.125**	**0.0625**	**0.0313**
2a	18	98.95±0.49	98.57±0.29	98.66±0.49	95.82±0.45	96.69±0.22	97.53±0.22	94.68±0.35	98.12±0.42	99.45±0.24	99.65±0.27
	48	99.05±0.29	98.81±0.11	98.90±0.23	97.23±0.14	98.80±0.07	98.82±0.11	98.19±0.11	99.16±0.18	99.12±0.17	99.02±0.27
2d	18	99.62±0.30	99.44±0.21	99.62±0.24	97.40±0.39	93.49±0.06	98.40±0.37	99.96±0.01	100±0.02	99.90±0.07	99.51±0.40
	48	99.39±0.44	99.06±0.15	99.41±0.46	99.14±0.44	98.22±0.33	99.22±0.47	99.62±0.24	99.43±0.32	99.34±0.06	99.38±0.45
3a	18	99.36±0.22	99.54±0.31	99.53±0.19	99.25±0.20	62.02±0.27	99.10±0.25	98.55±0.36	99.65±0.09	99.99±0.00	99.51±0.40
	48	99.22±0.21	99.63±0.45	99.29±0.33	99.57±0.44	97.60±0.22	99.16±0.49	99.16±0.55	99.19±0.29	99.76±0.18	99.38±0.27
3b	18	98.46±0.08	99.06±0.31	99.63±0.19	98.39±0.20	99.60±0.33	97.59±0.46	99.45±0.45	98.66±0.14	99.06±0.46	98.95±0.39
	48	98.26±0.05	99.08±0.18	98.84±0.10	98.87±0.18	98.65±0.18	98.95±0.08	98.79±0.09	98.92±0.05	99.12±0.14	98.94±0.04
3c	18	100±0.02	98.47±0.04	99.02±0.05	99.22±0.02	91.33±0.02	96.41±0.08	99.99±0.002	99.94±0.05	99.94±0.04	96.23±0.13
	48	98.74±0.14	98.75±0.19	98.93±0.15	99.24±0.38	99.10±0.20	98.74±0.12	99.04±0.16	98.90±0.09	98.83±0.09	99.00±0.04
3d	18	94.16±0.30	98.90±0.40	99.32±0.43	95.00±0.41	98.99±0.11	98.90±0.41	99.95±0.02	99.62±0.23	98.61±0.21	99.97±0.02
	48	98.34±0.13	99.05±0.19	98.50±0.06	98.60±0.11	98.69±0.06	98.89±0.08	98.96±0.11	99.13±0.08	99.03±0.08	99.17±0.05
4a	18	97.02±0.11	99.94±0.03	99.64±0.03	85.92±0.02	80.42±0.18	99.52±0.04	99.96±0.06	99.81±0.07	99.93±0.07	94.63±0.02
	48	99.31±0.20	98.82±0.04	99.15±0.20	98.84±0.12	98.87±0.08	99.59±0.08	99.13±0.20	97.95±0.03	99.55±0.03	98.98±0.03
4b	18	99.87±0.11	99.97±0.02	99.75±0.16	95.72±0.11	57.60±0.30	98.99±0.46	98.25±0.35	99.57±0.21	99.50±0.34	99.87±0.09
	48	99.44±0.78	99.39±0.38	99.45±0.46	98.30±0.07	96.58±0.05	99.18±0.48	98.68±0.18	98.96±0.44	99.03±0.34	99.56±0.61
4c	18	100±0.02	96.30±0.09	98.10±0.15	98.31±0.02	98.79±0.01	92.34±0.18	99.91±0.07	99.95±0.05	100±0.01	97.92±0.05
	48	99.35±0.21	98.81±0.04	98.97±0.11	99.61±0.17	99.36±0.22	99.32±0.33	99.24±0.29	98.92±0.11	99.28±0.30	99.12±0.29
4d	18	99.64±0.16	98.97±0.53	98.62±0.23	92.76±0.30	98.01±0.47	98.11±0.37	90.79±0.47	98.25±0.24	98.70±0.14	100±0.03
	48	99.20±0.23	98.97±0.31	98.91±0.05	97.16±0.12	99.02±0.34	98.83±0.09	98.01±0.17	98.94±0.18	99.00±0.15	99.12±0.08
5a	18	99.13±0.37	99.40±0.18	98.44±0.43	90.79±0.18	95.93±0.44	98.87±0.50	95.76±0.43	99.99±0.01	99.37±0.33	99.69±0.31
	48	98.96±0.10	99.02±0.13	98.91±0.17	97.06±0.06	98.87±0.08	98.96±0.18	98.01±0.20	99.01±0.05	99.26±0.28	99.23±0.24

5b	18	98.97±0.25	98.51±0.39	99.94±0.03	89.93±0.16	98.46±0.26	98.88±0.30	95.87±0.44	99.61±0.09	99.59±0.29	99.74±0.29
	48	98.82±0.21	98.86±0.10	99.01±0.22	97.05±0.10	99.04±0.10	99.08±0.07	98.72±0.37	98.94±0.01	99.11±0.22	99.34±0.08
5d	18	99.55±0.02	99.99±0.00	99.90±0.01	92.75±0.03	87.68±0.17	97.11±0.12	99.78±0.15	99.93±0.06	99.98±0.01	99.33±0.00
	48	99.28±0.26	99.17±0.23	99.25±0.08	99.07±0.04	99.17±0.23	99.06±0.14	99.02±0.16	99.24±0.05	99.19±0.23	99.20±0.26
6a	18	99.95±0.04	99.01±0.42	99.96±0.02	99.35±0.12	85.06±0.29	98.97±0.24	98.40±0.33	99.13±0.46	99.57±0.20	99.34±0.06
	48	99.65±0.30	98.86±0.25	99.68±0.48	99.70±0.14	97.51±0.04	99.31±0.43	98.70±0.08	99.18±0.49	99.12±0.15	99.12±0.11
6b	18	99.98±0.005	99.61±0.15	98.99±0.34	98.19±0.30	45.15±0.50	99.07±0.43	98.38±0.38	99.76±0.05	99.51±0.19	99.31±0.43
	48	99.37±0.43	99.14±0.57	98.95±0.33	98.95±0.55	96.34±0.36	99.16±0.53	98.95±0.30	98.72±0.17	98.79±0.22	98.81±0.23
6c	18	100±0.03	97.97±0.07	99.85±0.02	99.74±0.02	84.36±0.03	98.32±0.04	99.95±0.04	99.92±0.09	99.88±0.14	99.32±0.02
	48	98.78±0.09	98.86±0.11	99.07±0.10	99.12±0.16	98.78±0.08	99.00±0.07	98.87±0.07	98.85±0.13	98.80±0.17	99.14±0.12
6d	18	100±0.03	99.23±0.04	100±0.00	99.98±0.01	99.38±0.01	96.86±0.05	99.86±0.16	99.97±0.03	99.86±0.05	97.51±0.10
	48	98.83±0.14	98.84±0.17	99.05±0.16	99.41±0.31	98.86±0.12	98.84±0.14	99.09±0.14	98.82±0.09	98.78±0.06	99.27±0.29

Legend: [a]Amphotericin B at the concentration of 0.5 μg/mL was used as a control (inhibition % = 100).

Table 5. Fungicidal Activity of Tetrazole Derivatives against *C. albicans* 90028

Compound	*C. albicans* (CFU x 10^5) after treatment with tetrazole derivative at the concentration of 16 μg/mL (Tetrazole treated cells)	Untreated starting inoculum of *C. albicans* 90028 ATCC (CFU x 10^5) (Growth control cells)	Logarithm reduction (R) of *C. albicans* cells
2a	176	115	-0.18
2d	83	115	0.18
3a	196	115	-0.23
3b	126	565	0.65
3c	241	439	0.26
3d	177	565	0.51
4a	261	115	-0.34
4b	35	115	0.56
4c	203	439	0.34
4d	152	115	-0.08
5a	87	115	0.16
5b	432	115	-0.54
5d	119	115	-0.01
6a	59	115	0.33
6b	213	115	-0.23
6c	222	439	0.29
6d	282	439	0.19

Legend: Tetrazole derivative reducing the *C. albicans* cells at least for lg R≥3 was defined as fungicidal. Reduction was expressed as decimal log reduction separately using the formula: lg R = lg CFU/mL control cells – lg CFU/mL tetrazole treated cells. The fungicidal activity was determined using the microdilution method M27-A3. Accordingly, 50-μL aliquots from the wells of microplates containing tetrazole treated cells (PTW: tetrazole at the concentration of 16 μg/mL and yeast suspension) and the growth control cells (GCW: solvent DMSO or ethanol and yeast suspension) after 48-h incubation at 35°C were placed in volume of 100 μL onto Sabouraud dextrose agar plates after 10^4 dilution in PBS and incubated at 35°C for the next 48 h.

In Vitro and *In Vivo* Cytotoxicity of Tetrazole Derivatives

Due to the similar antifungal activity of all synthesised tetrazole derivatives the cytotoxicity of the following representative structures **2d**, **4b,** and **6a** derived from three different chemical syntheses was tested against the Caco-2 cell line *in vitro* after 18 h incubation. The data are summarized in Table 6 and show a relationship between the structure of the compound and the cytotoxicity. **2d** at 256 μg/mL (CC_{50}) was highly cytotoxic and reduced the Caco-2 viability to 63%. **2d** at 16 μg/mL displayed a 25%-reduction in viability *in vitro*. **6a** exhibited CC_{50} at 16 μg/mL against Caco-2 after 18-h treatment. Interestingly, toxicity of **6a** did not increase at the concentration of 256 μg/mL. Both **2d** and **6a** were non-

toxic at the concentration of 0.0313 μg/mL. Morpholine derivative **4b** did not reach CC_{50} at the tested concentrations. The close structurally related molecules with similar values (3.06-3.16) of log *P* (logarithm of the partition coefficient of inhibitor between n-octanol and water according to ChemBioDraw Ultra 13.0 software) exhibit remarkable differences in cytotoxicity. The replacement of the aliphatic chain with the morphine moiety lowered cytotoxicity.

Accordingly, tetrazole derivatives **2d** and **6a** were chosen for the *in vivo* toxicity assay. **2d** and **6a** had no effect on the larval survival *vs* the PBS-treated control ($p \leq 0.05$), and were therefore considered to be non-toxic at all the doses tested (Table 6).

Table 6 *In vitro* and *in vivo* Cytotoxicity of Tetrazole Derivatives **2d**, **4b**, and **6a**

Compound	Concentration (μg/mL)	Cytotoxicity assay			
		In vitro		*In vivo*	
		Toxicity of Tetrazole to Caco-2 cells (%)	Viability of Caco-2 cells (%)	Larvae Survival (%) after 96 h	Larvae Health Score
2d	256	63.27±0.22[a]	36.73±0.22	100±0.00	9±0.40
	16	25.49±0.53	74.51±0.53	100±0.00	9±0.60
	0.0313	0.00±0.52	100±0.52	100±0.00	10±0.00
4b	256	13.04±0.04	86.96±0.04	nd	nd
	16	27.73±0.24	72.27±0.24	nd	nd
	0.0313	18.76±0.29	81.24±0.29	nd	nd
6a	256	45.49±0.17	54.51±0.17	100±0.00	9±0.60
	16	50.46±0.10[a]	49.54±0.10	100±0.00	10±0.20
	0.0313	0.00±0.01	100±0.01	100±0.00	10±0.00
PBS-treated control		nd	nd	100±0.00	10±0.00

Legend: nd stands for not determined; [a] stands for cytotoxic effect (CC_{50}) of tetrazole against Caco-2. The analysis of Caco-2 cells' viability was assayed after 18-h treatment with compounds **2d**, **4b,** and **6a** respectively. Toxicity of **2d** and **6a** to *G. mellonella* larvae was assessed after 96-h incubation. Data are expressed as the mean ± SD of three independent experiments. All samples were tested in duplicate.

Antifungal Activity of Tetrazole Derivatives in the Presence of Sorbitol

To provide osmotic protection during the treatment with tetrazole derivatives, the cells were suspended in the isotonic RPMI medium containing sorbitol in the final concentration of 0.8 M. This allowed us to test whether exposure to sorbitol protects *C. albicans* against the tetrazole-induced inhibition. The tetrazole **6a**-induced growth inhibition was enhanced at 100 μg/mL notably after 7 days (Fig. 4 A, B). This result demonstrated the appearance of a surface barrier defect that increases corresponding with **6a**'s higher concentration. Compared with the untreated control cells, the cells exposed to sorbitol displayed substantial protection against

the **2d** tetrazole-induced inhibition (Fig. 4 C, D). Notably, the MIC values of both tetrazole derivatives tested, displayed no evident changes in the antifungal activity using sorbitol. Contrariwise, the antifungal effect of **2d** (especially at lower concentrations) was reversed in the medium containing sorbitol. Thus it is possible to consider the fungal cell wall as a target for the tested propionate esters.

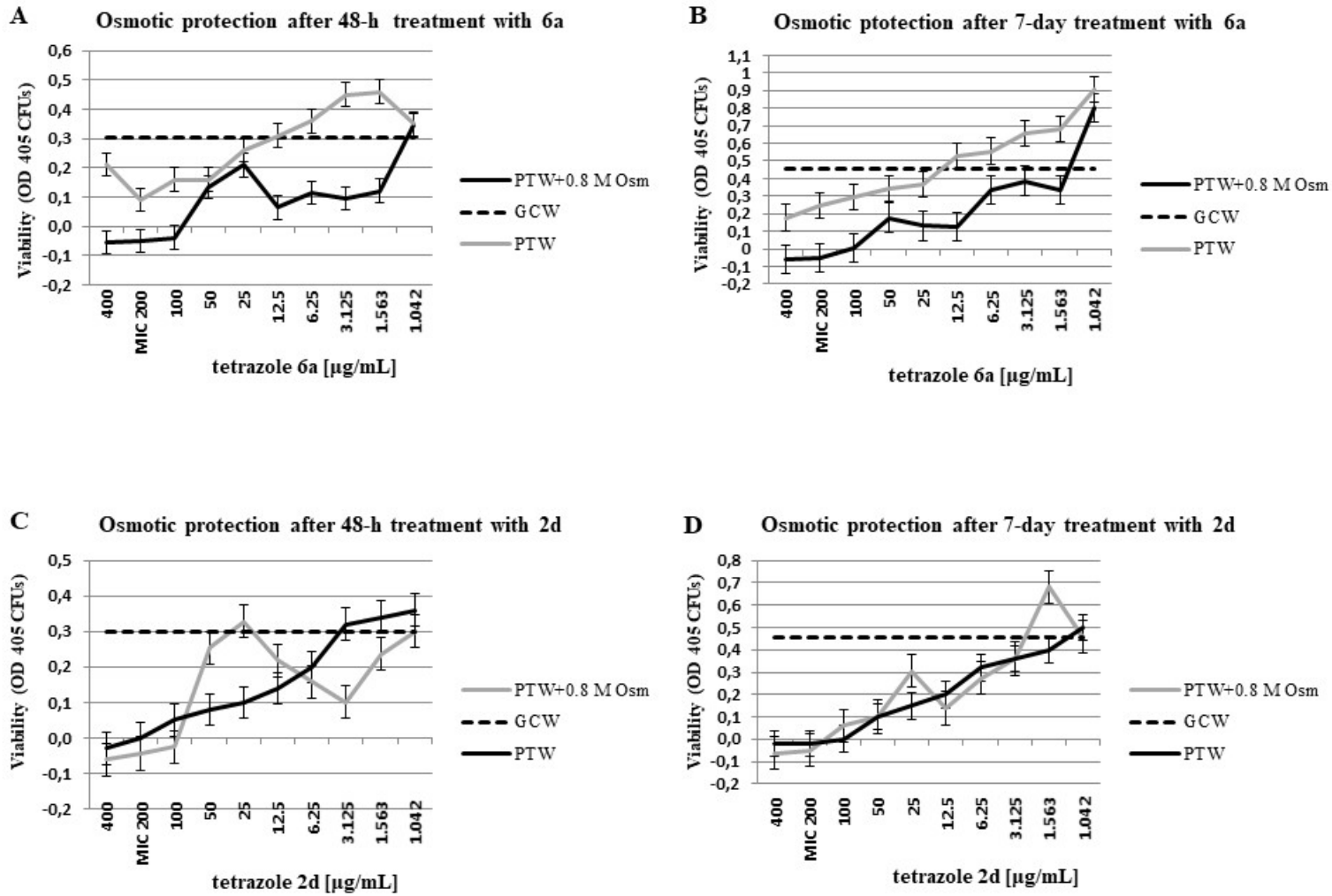

Fig. 4. Impact of Sugar Alcohol – Sorbitol (0.8 M) on the Antifungal Activity of Tetrazole Derivatives **2d** and **6a** Against *C. albicans*. **Legend**: PTW +0.8 M Osm stands for tetrazole + yeast suspension + 0.8 M sorbitol; GCW stands for yeast suspension + solvent; PTW stands for tetrazole + yeast suspension. MIC of **2d** and **6a** assessed with and without Osm protector was unaffected. The tests were performed with the microdilution method M27-A3 in triplicate, and the plates were incubated at 35°C for 7 days. Reading was performed after 2 and 7 days respectively.

Tetrazole Derivatives Display Antagonism in Combination with Fluconazole

In the case of the tetrazole derivatives tested on their own, as described above, due to the absence of a clear endpoint in the range of the concentrations tested using M27-A3 method, in order to calculate the FIC index the assumption was made of the endpoint as >16 μg/mL. As shown in Table 7, Flc alone had good antifungal effect towards the reference strain displaying MIC and endpoint at 0.25 μg/mL (determined visually and spectrophotometrically using the microdilution method M27-A3). Next, the effects of tetrazole derivatives **2d**, **4b** or **6a** combined separately with Flc against *C. albicans* were investigated and the percentage of growth inhibition was determined (Table 8). The endpoint value of Flc increased 5-fold when combined with the partner tetrazole **2d**. Surprisingly, the combination of **4b** and **6a** with Flc respectively produced unidentified MICs. Nevertheless, taking the endpoint values as >80 μg/mL for Flc, **4b**, and **6a**, the FIC indexes of all the tested combinations were >1, thus resulting in antagonism (data not shown). Subsequently, these results were confirmed by testing the metabolic activity of *C. albicans* cells treated with tetrazoles combined with Flc with the use of the XTT method (Table 9). When these agents were tested in their combinations, Flc reduced the cells viability at >90% at 1.25 μg/mL. The active concentrations of tetrazoles combined with Flc were respectively 20 μg/mL for **4b** and 80 μg/mL for both **2d** and **6a** (50%-reduction in viability). Based on the XTT results, the recalculated FIC indexes of all the combinations tested fit the definition of antagonism (Table 10).

Table 7 Antifungal Activity of Fluconazole Against the Reference *C. albicans* Strain ATCC 90028

Time (h)	Fluconazole (μg/mL)											
	64	**32**	**16**	**8**	**4**	**2**	**1**	**0.5**	**0.25**	**0.125**	**0.0625**	**0.0313**
18	100	100	100	100	100	100	100	100	100	100	100 [a]	99.74
48	100	100	100	100	100	100	100	100	100 [a]	99.96	99.18	98.89

Legend: [a] indicates total growth inhibition named endpoint = 100% calculated based on the growth rate assessed spectrophotometrically (OD_{405}) and visually MIC_T; data are expressed as means ± SD.

Table 8 Growth Inhibition in the Checkerboard Microtiter Plate Testing the Combination of Fluconazole with Partner Tetrazole Derivatives **2d**, **4b,** or **6a** Against *C. albicans* ATCC 90028 After 48 h

Partner tetrazole		Fluconazole (μg/mL)						
Concentration (μg/mL)	**Name**	**80**	**40**	**20**	**10**	**5**	**2.5**	**1.25**
80	**2d**	99.78	99.79	99.74	99.78	99.27	99.67	100 [a]
	4b	99.54	99.21	99.71	99.80	97.80	99.54	98.77
	6a	99.61	99.34	99.59	99.84	99.18	99.77	99.97
40	**2d**	99.54	99.43	99.53	99.59	98.95	99.14	99.93
	4b	99.59	99.45	99.55	99.69	98.83	99.77	99.57
	6a	99.58	99.45	99.54	99.53	98.93	99.74	99.56
20	**2d**	99.33	99.34	99.69	99.73	99.02	99.25	100
	4b	99.26	98.99	99.10	99.32	98.27	99.31	98.75
	6a	99.25	99.29	99.50	99.52	98.72	99.63	99.79
10	**2d**	99.43	99.29	99.61	99.67	98.90	99.41	99.86
	4b	99.21	98.78	98.99	98.99	98.12	98.46	97.81
	6a	99.49	99.34	99.46	99.41	98.97	99.62	99.72
5	**2d**	99.34	99.25	99.67	99.66	98.81	99.14	99.79
	4b	99.47	99.15	99.16	98.80	98.69	98.90	98.77
	6a	99.61	99.51	99.58	99.57	99.12	99.77	99.71
2.5	**2d**	99.49	99.32	99.53	99.75	98.94	99.42	100
	4b	99.19	98.91	98.82	99.09	98.33	98.48	98.95
	6a	99.54	99.46	99.52	99.49	99.08	99.77	99.79
1.25	**2d**	99.49	99.16	99.58	99.66	98.74	99.64	99.71
	4b	99.54	99.36	99.46	99.59	99.86	99.23	99.02
	6a	99.51	99.46	99.65	99.65	98.99	99.20	99.81

Legend: [a] indicates total growth inhibition 100% – endpoint. In case of **4b** and **6a** combination with **Flc** no endpoint was identified. Therefore, endpoint was taken as the highest concentration of 80 μg/mL to calculate the FIC index.

Table 9 Metabolic Activity of *C. albicans* ATCC 90028 After 48 h Treatment with the Combination of Fluconazole with Partner Tetrazole Derivatives **2d**, **4b**, or **6a**

Metabolic activity (%) of *C. albicans* cells treated with agents' combination								
Partner tetrazole		**Fluconazole (μg/mL)**						
Concentration (μg/mL)	**Name**	**80**	**40**	**20**	**10**	**5**	**2.5**	**1.25**
80	**2d**	53.22	89.73	70.42	73.98	100	59.43	2.60 [a]
	4b	73.44	100	50.83	11.87	100	78.22	100
	6a	40.00	97.37	73.11	52.64	100	64.31	41.98 [a]
40	**2d**	63.62	100	74.10	70.86	100	75.66	13.59
	4b	66.33	95.31	54.14	28.26	100	26.03	40.06
	6a	55.99	100	54.82	56.45	100	61.61	66.60
20	**2d**	81.77	82.92	67.85	68.01	99.55	81.50	0.00
	4b	69.42	93.50	61.69	46.94 [a]	100	71.88	76.07
	6a	94.76	99.65	57.34	59.93	100	80.61	90.68
10	**2d**	80.34	100	87.40	75.42	100	79.69	73.65
	4b	89.30	100	93.01	99.02	100	100	100
	6a	77.26	94.14	70.81	76.18	100	71.14	90.58
5	**2d**	77.27	86.34	73.79	66.60	100	68.03	79.99
	4b	88.19	100	93.31	81.48	100	100	100
	6a	71.92	94.92	67.66	69.35	100	80.73	88.02
2.5	**2d**	80.42	97.62	68.53	64.55	100	75.77	0.00
	4b	84.01	100	86.25	85.87	100	100	100
	6a	72.63	92.82	67.39	71.01	95.38	82.62	90.20
1.25	**2d**	62.42	81.57	60.65	62.08	100	71.55	86.44
	4b	100	100	100	100	100	100	74.26
	6a	66.82	86.85	62.20	74.44	100	75.73	87.00

Legend: [a] indicates inhibition of metabolic activity <50%; Because of the residual turbidity observed at supra – endpoint of compounds' combination (tetrazole **2d** combined with Flc) indicating an incomplete metabolic activity inhibition, accordingly, the lowest concentration could therefore not be used as an endpoint in this experimental setting. We selected the highest concentration reducing metabolic activity of <50%.

Table 10 Effects of Tetrazole Derivatives **2d**, **4b**, and **6a** in Combination with Fluconazole Against *C. albicans* Assessed using XTT and Growth Inhibition (Microdilution Method M27-A3)

No. of combination	Compound	MIC[a] (μg/mL)	Combination MIC[b] (μg/mL)	FIC	Total FIC index	Effect
1	Fluconazole	0.25	1.25	5.0	>10	antagonism
	2d	>16	80	>5.0		
2	Fluconazole	0.25	10	5.0	>6.25	
	4b	>16	20	>1.25		
3	Fluconazole	0.25	1.25	5	>10	
	6a	>16	80	>5		

Legend: [a] indicates total growth inhibition (clear end point, MIC_{TI}); [b]stands for metabolic reduction; Total index means sum up of FIC of Flc and appropriate tetrazole.

Impact of Tetrazole Derivatives 2d, 4b and 6a on Adhesive Properties of *C. albicans*

As shown in Table 11, the cells pre-treated with tetrazole derivatives **2d**, **4b** and **6a** at 256 μg/mL showed significant changes in the adhesion properties to Caco-2, when compared with the non-treated control ($p \leq 0.05$). Of these, **6a** at 256, 16 and 0.0313 μg/mL inhibited cells' adhesion respectively as follows: 2.5-, 2.9- and 2.7-fold ($p \leq 0.05$, compared to non-treated control). The remaining compounds **2d** and **4b** at 256 μg/mL significantly increased the attachment of fungal cells to Caco-2 *vs* untreated counterparts ($p \leq 0.05$).

Table 11 The Percentage of Adhesion of *C. albicans* Cells to Caco-2 Cell Line After Pre-treatment with Compounds **2d**, **4b**, and **6a**

Compound	Concentration (µg/ml)	Adherent cells (%)	Reduction of cell adherence (%)
	256	**91.58±4.14**	**I**
2d	16	35.77±5.01	I
	0.0313	**48.14±6.54**	**I**
	256	**48.29±5.38**	**I**
4b	16	25.71±8.15	14.18
	0.0313	37.93±8.46	I
	256	**12.22±3.85**	**59.12**
6a	16	**10.36±3.97**	**65.41**
	0.0313	**10.91±1.84**	**63.41**
Non-treated control cells		29.96±4.43	nc

Legend: I stands for increased adherence properties of *C. albicans* compared to the untreated control cells; nc stands for not considered. Adherence was expressed as a percentage of the total number of cells added (non-treated control cells). Data are expressed as the mean ± SD of three independent experiments. Values in bold indicate significantly affected adhesive properties compared to non-treated control ($p \leq 0.05$).

Programmed Biofilm Cell Death under 6a

We assessed the structural and functional changes taking place during the cell death under the tetrazoles tested using different methods whose results are described below. In line with Cevik and Dalkara [39], we showed that under **6a**, the same biofilm cells can display both early apoptotic and necrotic features. Two dyes: PI and AO of both pathways were studied *in vitro*. PI showed no toxic effects against the **6a**-untreated biofilm. In the present study we demonstrated the membrane-impermeable PI which marked necrotic cell death in the biofilm after treatment with **6a** at three different concentrations. In biofilm *in vitro* under **6a** there were cells labelled with PI and AO. The PI-labelled cells with a leaky membrane displayed necrotic features such as the pyknotic nuclei (Fig. 5 E). It is clear that the membrane was disrupted at the tested concentrations: 256, 16, and 0.03 µg/mL. Thus the PI-stained cells might have gone to necrosis after the DNA fragmentation which is shown below. Under **6a** (at all the tested concentrations) all the biofilm cells were labelled with AO, indicating early apoptotic cells. These cells could have gone to the final stage apoptosis due to the loss of the membrane integrity. We concluded that **6a** caused biofilm cell death with the contribution of apoptosis and necrosis.

As it was shown in Fig. 5, for biofilm treated with 0.03 μg/mL the staining pattern resulting from the use of PI and AO dyes makes it possible to distinguish dead and early apoptotic cell population with fluorescence microscopy. The AO assay showed early apoptotic cells with bright green nucleus with condensed chromatin (Fig. 5 F, I, L). In the cells treated with 0.03 μg/mL, as the cell membrane was compromised, PI gained access to the nucleus rendering red fluorescence. Microscopic analysis of the biofilm treated with 256 μg/mL confirmed **6a-**caused chemical damage to the cells. PI staining showed that **6a** at 256 μg/mL caused the cell death – the necrotic cells fluorescence red. AO staining showed apoptotic cells with a bright green nucleus. Under 16 μg/mL, PI labelling indicated necrotic biofilm cells that lost their membrane integrity. AO-labelled cells displayed late apoptotic features such as condensed chromatin.

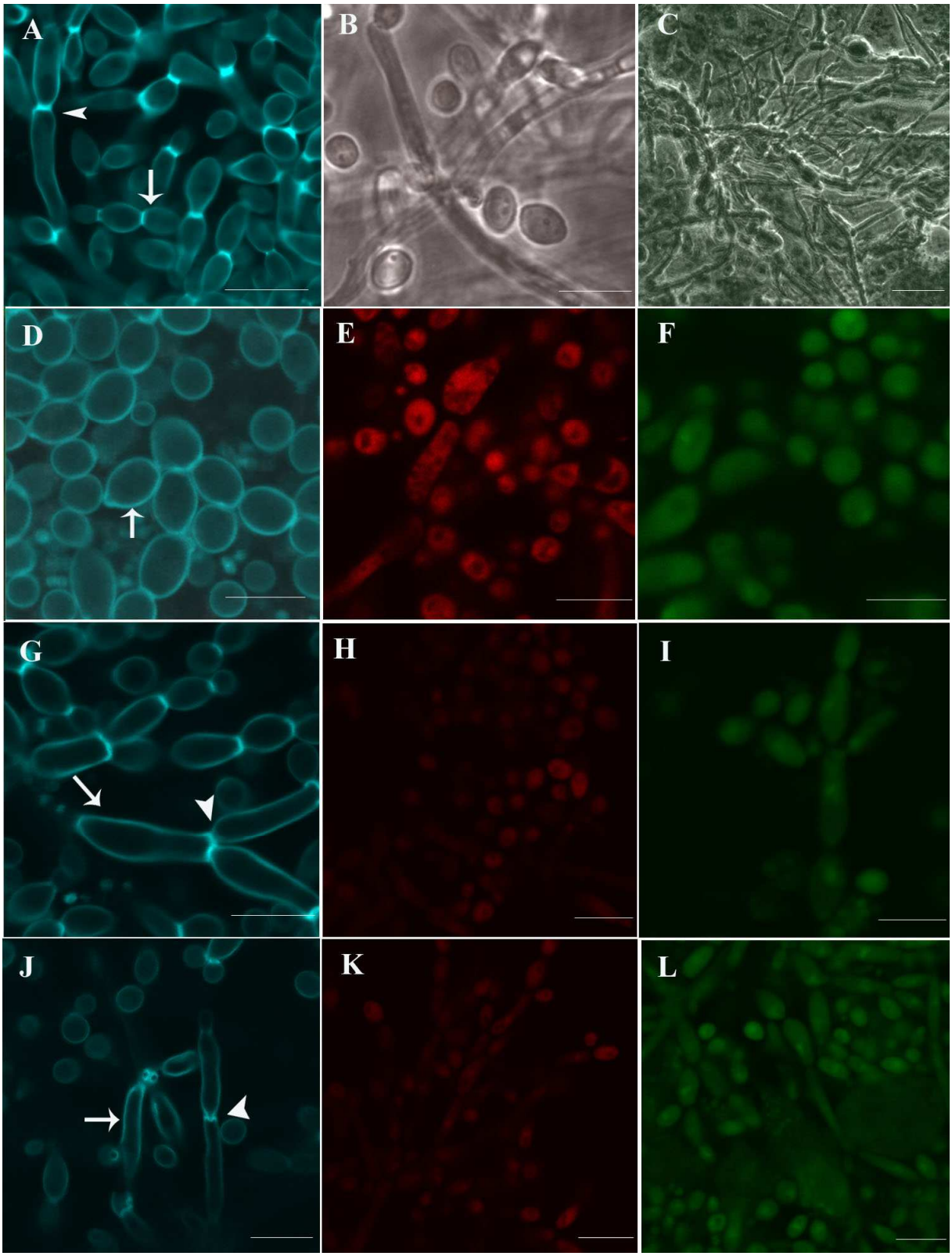

Fig 5. Fluorescence Imaging Assay for Studies on the Programmed Biofilm Cell Death.

Legend: Unfixed *C. albicans* mature biofilm cells growing on the TR146 monolayer for 18 h are stained using a negatively charged fluorophore Propidium iodide PI (5µg/mL) to test for membrane integrity and cell viability as well as with Acridine orange AO crossing the membrane of viable and early apoptotic cells. **(A-C)** Untreated control biofilm cells labelled using calcofluor white CFW **(A)** reveal typical distribution of chitin rich content in true hyphal septa (arrowhead) and in fragile septa (arrow) between elongated blastoconidial cells forming

pseudohyphae. **(B)** The untreated cell membrane's integrity prevents PI dye diffusion – viable cells remain unstained. Phase contrast in combination with fluorescence were used due to the lack of dying effect in fluorescence image applied on its own. **(C)** AO-penetrated the control cells fluorescing green when the dye bound to DNA. Phase contrast and fluorescence combination. (**D-F**) Treatment with **6a** at 256 µg/mL for 18 h. **(D) 6a**-treated biofilm is impaired in morphogenesis, chitin-enriched blastoconidia showing CFW staining around the cell surface (arrow). **(E)** Necrotic cells increase in volume and show red fluorescence, staining is localized asymmetrically with the cells. In comparison to the control cells, **6a**-treated cells at 256 µg/mL reveal much higher intensity resulting from IP intense nuclear labelling. **(F)** Early apoptotic cells exhibit dense bright green areas of chromatin condensation under **6a** at 256 µg/mL. **(G-I)** Treatment with **6a** at 16 µg/mL. **(G)** Cells display chitin-rich septa stained with CFW (arrowhead) and staining around the cells occurs (arrow). These results indicate that **6a** at 16 µg/mL affects surface integrity less compared to its conc. of 256 µg/mL. **(H)** PI staining reveals labelling of cytoplasm in necrotic cells under **6a**. **(I)** Morphological changes in early apoptotic cells: nucleus showed bright green fluorescence with AO staining. **(J-L)** Treatment with **6a** at 0.03 µg/mL. **(J)** CFW binds to polysaccharide-chitin located at septal areas (arrowhead) and around the cell wall (arrow). The bright bluish fluorescence indicates a higher content of chitin in the cell wall of 0.03 µg/mL-treated biofilm. **(K)** 0.03 µg/mL-toxic effect on biofilm - red fluorescence indicates necrotic cell population. **(L)** 0.03 µg/mL-treated early apoptotic cells exhibiting bright green intensity. Bars = 20 µm.

We observed morphological distinctions between the cell death in apoptosis and necrosis under the tested tetrazole derivatives. Firstly, the gel electrophoresis-based method testing the **6a**-treated cells at 256 µg/mL, did not detect DNA ladder but its total denaturation comparable to the control DNA (extracted from the cells treated with 100°C for 10 min) contrary to the untreated cells (data not shown). The lack of apoptotic changes in the **6a**-treated cells was supported by the negative results of the comet assay indicating necrosis induced by the tetrazole tested under the same conditions. While DNA remained inside the cell, the cytoplasmic swelling and chromatin condensation were noted.

Necrosis-like Programmed Cell Death - Flow Cytometry

Table 12 outlines accidental cell death (necrosis) under tetrazole derivatives **2d** and **6a** at 16 µg/mL. The viability of control protoplast was approximately at 59.19%±11.0 depending on the log-phase of culture growth and the generation procedure [34]. The protoplasts produced for the study were able to regenerate on Sabouraud agar after incubation for 18 h at 30°C. Both untreated and **6a**-treated protoplasts were recovered respectively in uncountable (carpet-like growth) and countable numbers of 632 CFU/mL PBS. The latter recovery resulted from **6a**'s fungistatic activity, which can be reversible without agent's influence. The number of cellular suicide generated by tetrazoles at conc. of 16 µg/mL was higher, 89.92-97.03% *vs* untreated protoplasts (40.48%, Table 12).

Table 12 Necrosis-like Programmed Planktonic Cell Death – Flow Cytometry Analysis

Samples	Compound concentration (μg/mL)	% of cells with each result after 18 h of exposure[a]			
		Necrosis	Late Apoptosis	Viable Cells	Early Apoptosis
Control protoplasts	nt	40.48±16.81	0.20±0.28	59.19±11.0	0.13±0.06
2d-treated protoplasts	16	89.92±4.81	0.23±0.12	1.85±0.07	8.00±8.20
6a-treated protoplasts	16	97.03±0.88	1.20±0.50	1.67±0.88	0.1±0.00

Legend: [a] The data are mean percentages ± standard deviations; nt stands for not tested

Evaluation of 6a's and 2d's Effect on Ergosterol

Compounds **6a** and **2d** were tested to investigate their ability to form the complexes with ergosterol. Fig. 6 shows graphs representative of these results, suggesting that these compounds had no interaction with ergosterol. The MIC values estimated visually suited the growth inhibition curves delineated spectrophotometrically (A_{405} and the reference A_{600}). In the presence of exogenous ergosterol MIC=64 μg/mL of **6a** was lower compared with the control. Compound **6a** tested without the exogenous ergosterol exhibiting MIC=128 μg/mL (Fig. 6A). Compound **2d** also did not show a specific interaction with ergosterol (2xMIC reduced *vs* MIC assessed for **2d** alone; Fig. 6B). Contrariwise, for **ITR** in the presence of the exogenous ergosterol 2xMIC was noted *vs* its control without ergosterol (Fig. 6D). In the tested concentration range for AmB depicted in Fig. 6C, an inverse relation between AmB+Ergosterol (MIC=0.24 μg/mL) and AmB alone (MIC=0.03 μg/mL) was noted, strongly suggesting its affinity to ergosterol. No MICs were observed when AmB at the concentration range from 0.24 to 125 μg/mL was tested both in the presence or absence of ergosterol (data not shown).

A

Growth inhibition curves of *C. albicans* SC5314 treated with 6a

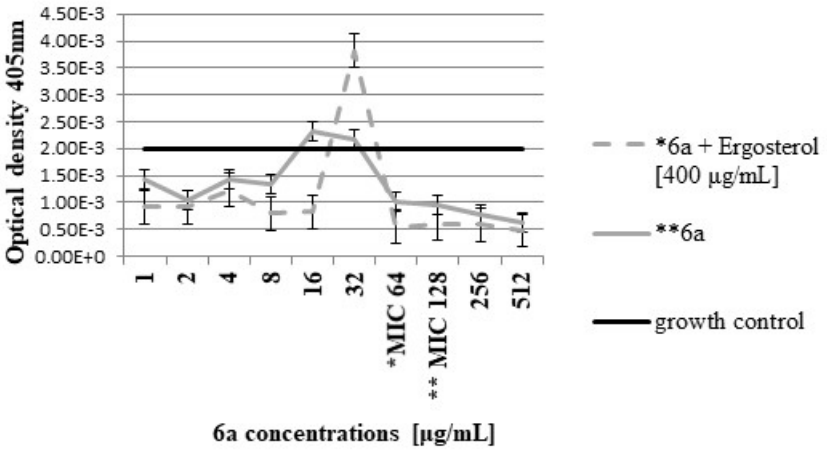

B

Growth inhibition curves of *C. albicans* SC5314 treated with 2d

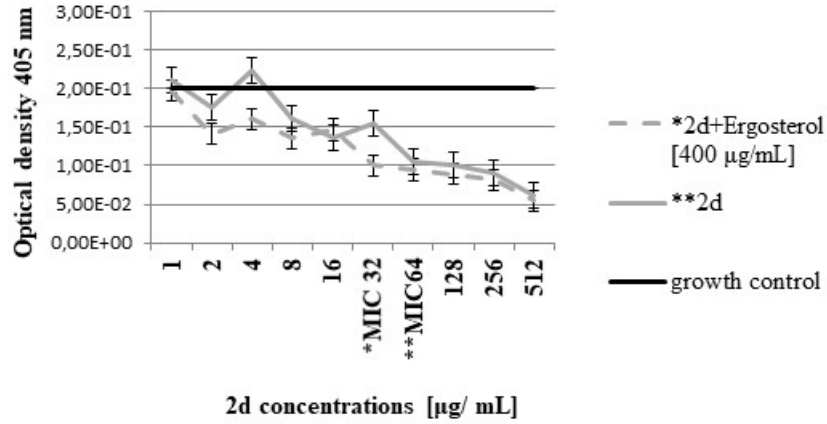

C

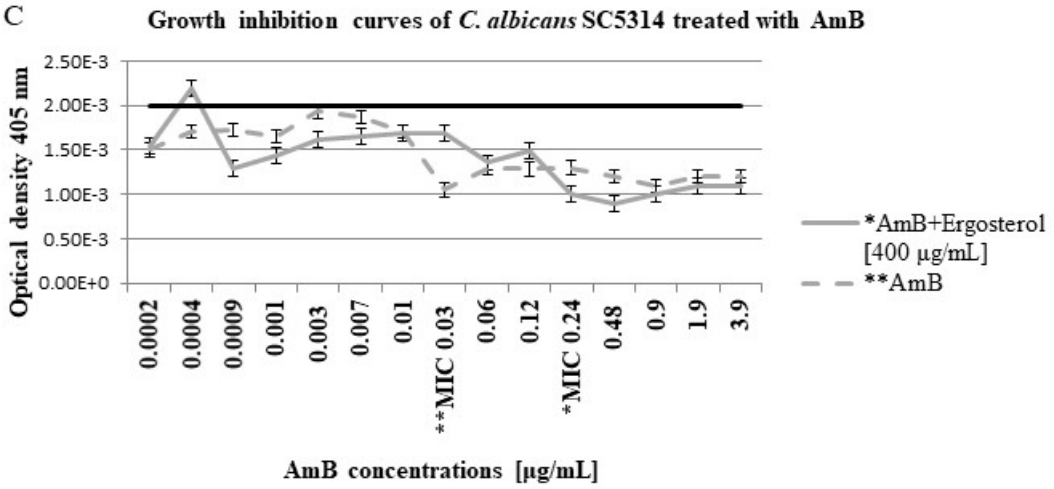
Growth inhibition curves of C. albicans SC5314 treated with AmB
Optical density 405 nm
2.50E-3
2.00E-3
1.50E-3
1.00E-3
0.50E-3
0.00E+0
0.0002
0.0004
0.0009
0.001
0.003
0.007
0.01
**MIC 0.03
0.06
0.12
*MIC 0.24
0.48
0.9
1.9
3.9
AmB concentrations [µg/mL]
*AmB+Ergosterol [400 µg/mL]
**AmB

D

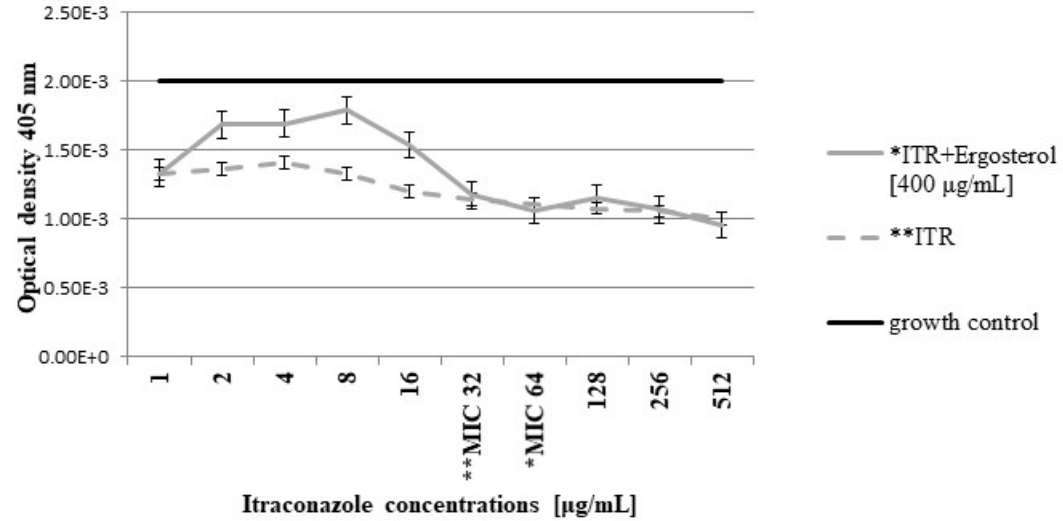
Growth Inhibition Curves of C. albicans SC5314 Treated with ITR
Optical density 405 nm
2.50E-3
2.00E-3
1.50E-3
1.00E-3
0.50E-3
0.00E+0
1
2
4
8
16
**MIC 32
*MIC 64
128
256
512
Itraconazole concentrations [µg/mL]
*ITR+Ergosterol [400 µg/mL]
**ITR
growth control

Fig. 6. Interactions of the New Tetrazole Derivatives with Exogenous Ergosterol. **Legend**: Binding assay with ergosterol was performed by mixing the exogenous ergosterol at final concentration of 400 µg/mL with the fungal suspension prepared according to the method M27-A3, as it was indicated respectively: (A) **6a**+Ergosterol [400 µg/mL], (B) **2d**+Ergosterol [400 µg/mL], (C) **AmB**+Ergosterol [400 µg/mL], (D) **Itraconazole**+Ergosterol [400 µg/mL]. The MIC values for the following tested compounds separately with or without ergosterol: **6a** (A), **2d** (B), **AmB** (C), and **Itraconazole** (D) were determined by eye on the 96-well plate after incubation of 48 h at 35°C. The experiments were performed in triplicate. While AmB showed no visible MIC at the range of concentrations: 0.24-125 µg/mL (data not shown), we tested the concentration range from 0.0002 to 3.9 (C). **6a** (A) and **2d** (B) displayed no sterol binding as their resulting MICs at the presence of exogenous ergosterol were lower *vs* their control without ergosterol. This demonstrated that the synthesized tetrazoles did not act *via* the action mode and inhibition of the fungal growth by binding specifically to ergosterol. In strong contrast to these new tetrazole derivatives, AmB's (C) and Itraconazole's (D) MICs were enhanced 8xMIC and 2xMIC respectively. AmB stands for Amphotericin B, ITR stands for Itraconazole ,

Efficacy of 6a in *G. mellonella* Infected with *C. albicans*

In vivo efficacy of **6a** at 16 μg/mL against *C. albicans* was evaluated using *G. mellonella* as non-mammalian host model. Compound **6a** was injected directly into the hemocoel, which resembles the conventional administration route used in mammalian models [13]. Single treatment doses of **6a** administered 30 min and 1 h before inoculation with *C. albicans* significantly improved larval survival (Fig. 7A). Improvements in larval survival were also observed in the groups treated with **6a** at 30 min and 1 h post *C. albicans* inoculation. Compound **6a** efficiently inhibited infection and increased the larvae survival up to 18 h ($p \leq 0.05$); whereas the protective antifungal activity of **6a** observed after 48 h failed to achieve statistical significance (Fig. 7A).

In order to obtain more subtle differences in the larvae heath status, each wax worm was scored according to the criteria of Loh *et al.* [14], where a healthy wax worm typically scores between 9 and 10, and an infected (dead) one scores 0. As shown in Fig. 7B, **6a** increased the health score of the infected wax worms in all the time intervals tested. At 18-h incubation, the larval health status significantly increased in the groups pre-treated with **6a** prior to *C. albicans'* inoculation and in the group treated with **6a** at 30 min post infection ($p \leq 0.05$). The beneficial effects of **6a** administered at these time intervals were sustained after 48 h. In contrast, **6a** administered 1 h after infection significantly increased the larval health score after 18 h, yet it failed to maintain statistical significance after 48 h (Fig. 7B).

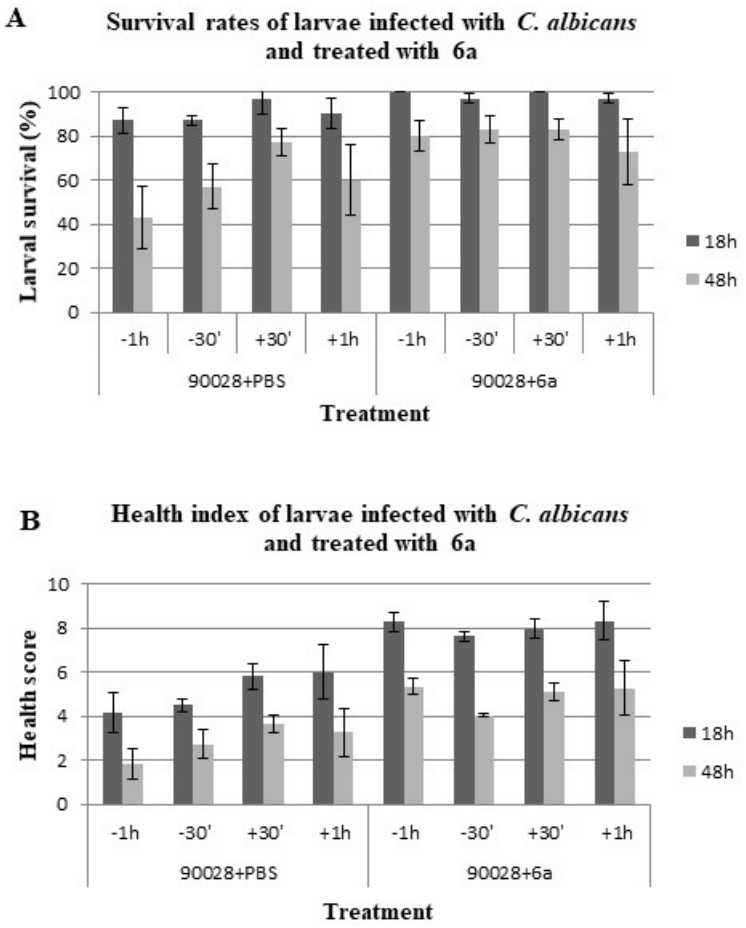

Fig. 7. Efficiency of **6a** at 16 μg/mL in Treatment of *G. mellonella* Larvae Infected with *C. albicans*. (A) Survival rate (%) of larvae expressed as Mean ± SEM. (B) Health index scores of infected wax worms over 48 h post treatment with **6a** (Mean ± SEM).

Discussion

After an extensive literature search [4, 40-49], we state that it is the first attempt to assess the antifungal activity against *C. albicans* of 1-(3-chloropropyl)-5-aryltetrazoles, propionate esters bearing tetrazole moiety and 5-aryltetrazoles containing morpholine scaffold. Interestingly, we found that the anti-*C. albicans* potential of the tetrazole derivatives seems to be independent of the kind of substituents on benzene ring and its orientation (Fig. 1-3 and Table 1-3). While generally azoles affect ergosterol biosynthesis [50], we suggested another mechanism for these newly synthesized tetrazoles. Importantly, the results only showed the fungistatic activity of the terazoles tested, thus the selected derivatives differing in chemical synthesis were characterized in more detail in *view* of their action mode as discussed below. In the study we demonstrated that tetrazoles **6a** and **2d** inhibit *C. albicans* by permeabilizing or not permeabilizing the plasma membrane respectively. The relation of **6a**'s and **2d**'s interaction with ergosterol to the MIC values is shown in Fig. 6 (A and B), at cell density corresponding to an A_{405} of 0.2. Fig. 6 shows an inverse relation between MIC of **6a** and **2d** respectively in the presence of ergosterol *vs* without it, but the effect was opposite to the control AmB and ITR presented here and described in [51]. However, MIC of **6a** and **2d** was changed in the presence of exogenous ergosterol suggesting that the compounds, especially **6a** can interact with the membrane. This was also observed in our data related to the cell death primary mechanism (Table 12 and Fig 5). As shown in the flow cytometry analysis, **6a** can damage the fungal membrane by acting with elements other than ergosterol. The generation of necrotic cells under **6a** detected by dual annexin V/IP staining using flow cytometry was further confirmed by increase in the biofilm necrotic cells' volume showing red fluorescence under confocal microscopy. The **6a**-treated cells appeared to be in the process of disintegration (Fig. 5). Morphological changes as swollen and larger dead cells under **6a** stained with IP intercalates with DNA following its passing exclusively disorganized or damaged cell membranes. Necrosis-like programmed cell death appeared under **6a** beyond its concentration range tested, however the structure of **6a**-membrane complex is unknown. If the tetrazole does involve permeabilization, it can be acting *via* oxidative damage of membrane structure which cannot perform its functional effects [50, 52]. It may be assumed that **6a** can produce holes in the membrane enabling annexin V to enter and bind to the phosphatidylserine of the inner membrane leaflet (false positive results in cell death interpretation). On the other hand, the fluorescence micrographs showed the necrotic-like programmed death of biofilm cells increased in volume (Fig. 5), which can release intracellular components [53]. Regardless of the latter, application of other methods

confirmed the cells necrosis under **6a**. Although the XTT assay cannot distinguish between apoptotic and necrotic cells [52, 54], it clearly indicated in our study the mitochondrial damage under **6a** combined with Flc (2.63-60% cell cytotoxicity at 80 μg/mL). Moreover, the *Candida* cells' adhesion reduction under **6a** to human epithelial cells *in vitro* confirmed yeast cells necrosis compared to an increased adhesion under **2d**.

As distinct from **6a** and other azoles studied so far [40-41, 55-56], **2d** displayed a mechanism targeted at the cell wall. It is very likely that 3-chloropropyl attached to aryltetrazole in **2d** is slightly directed at the function of the wall in *C. albicans* cells. This may be a possible explanation for the differences between **6a**'s and **2d**'s action mode and an increased adhesion under the latter. Concomitantly, the fluorescence micrographs of the CFW-stained cells allowed us to observe an irregular deposit of chitin in *C. albicans* cells treated with **6a** (Fig. 5). In line with the observations of Escalante et al. [57], the membrane damage produced by **6a** triggers chitin synthesis as a mechanism of defence to the fungal cell. Neither **6a** nor **2d** fragmented DNA (in alkaline comet assay) except for the disrupted membrane integrity under the first one tested. This can be due to dead cells which disappear as the heavily denaturated DNA disperses [31]. The **6a**-treated necrotic cells generated total DNA denaturation using agarose gel electrophoresis (data not shown). These data appear to be consistent with the findings of others authors [31, 58] that mitochondrial and membrane damage cause DNA denaturation *via* necrosis.

6a's ability to increase cell membrane permeability can explain the deleterious effects observed on the mature biofilm morphology and viability (Fig. 5). The ability of the tetrazoles to lyse human cells Caco-2 (toxic effect) was slight and it depended on the structure of the tetrazoles. **2d** showed toxicity against Caco-2 (CC_{50} at 256 μg/mL) which does not corroborate the findings *in vivo* using *G. mellonella*. Moreover, we applied this experimental host model [12, 59] to investigate efficiency of **6a** against the *C. albicans* infection. In the study, **6a** at 16 μg/mL failed to significantly improve the survival of wax worms previously infected with *C. albicans*. However, the pre-treatment of larvae with **6a** at 16 μg/mL efficiently protected them against subsequent *C. albicans* infections ($p \leq 0.05$). Our findings suggest that **6a** could be considered as a lead structure for a potential development of antifungal agents that can be used successfully to prevent invasive candidiasis.

Conclusions

The series of novel tetrazole derivatives using simple and not expensive methods was obtained. As well *N*-alkylation as Michael-type addition took place smoothly upon treatment appropriate 5-aryltetrazole with 1-bromo-3-chloropropane or ethyl acrylate, respectively.

Comparing the yields of these reactions significantly better results were obtained in Michael-type additions. All compounds were identified by ^{1}H NMR, ^{13}C NMR, IR and HRMS spectra. *C. albicans* cells showed pleiotropic response to **6a**. The mitochondrial permeability transition-dependent necrosis following membrane damage under **6a** was observed. Compound **2d** altered the synthetic route of *Candida*'s cell wall formation. Thus the synthesized tetrazole derivatives do not act as conventional azole drugs (including imidazoles, triazoles, and tetrazoles) targeted at ergosterol biosynthesis. In this case, new tetrazole derivatives with the novel action mode can circumvent an appearance of antifungal-resistant strains. As the compounds examined in this study have fungistatic and slight anticancer activity (anti-proliferative activity against Caco-2), these results indicate that they are worthy of further studies. Other combinations of these compounds with antimycotics are now encouraged for further investigations in order to improve their efficiency and manage toxicity in clinical use.

Conflict of interest

There is no conflict of interest.

Acknowledgement

MS and MG were financed by: (1) National Science Centre (No. DEC-2011/03/D/NZ7/06198; No. 2014/15/N/NZ6/03710), and (2) National Institute of Public Health-National Institute of Hygiene (No. 9/EM/2016). EŁ-Ch was financed by Warsaw University of Technology, Faculty of Chemistry.

References:

[1] A. Ahmad, J. Molepo, M. Patel, Challenges in the development of antifungal agents against *Candida*: scope of phytochemical research, *Curr. Pharm. Des.* 22 (2016) 4135-4150. Doi: 10.2174/1381612822666160607072748.

[2] L.V. Myznikov, A, Hrabalek, G.I. Koldobskii, Drugs in the tetrazole series, *Chem. Heterocycl. Compd.* 43 (2007) 1-9. Doi: 10.1007/s10593-007-0001-5.

[3] V.A. Ostrovskii, R.E. Trifonov, E.A. Popova, Medicinal chemistry of tetrazoles, *Russ. Chem. Bull.* 61 (2012) 768-780. Doi: 10.1007/s11172-012-0108-4.

[4] C. X. Wei, M. Bian, G.H. Gong, Tetrazolium compounds: synthesis and applications in medicine, *Molecules* 20 (2015) 5528-5553. Doi: 10.3390/molecules20045528.

[5] S.Y. Zhang, D.J. Fu, X.Y. Yue, Y.C. Liu, J. Song, H.H. Sun, H.M. Liu, Y. B. Zhang, Design, synthesis and structure-activity relationships of novel chalcone-1,2,3-triazole-azole derivatives as antiproliferative agents, *Molecules* 2016; 21: 653. Doi: 10.3390/molecules21050653.

[6] L.L. Dai, H.Z. Zhang, S. Nagarajan, S. Rasheed, C.H. Zhou, Synthesis of tetrazole compounds as a novel type of potential antimicrobial agents and their synergistic effects with clinical drugs and interactions with calf thymus DNA, *Med. Chem. Comm.* 6 (2015) 147-154. Doi: 10.1039/c4md00266k.

[7] G. Ramage, J.L. López-Ribot, Techniques for antifungal susceptibility testing of *Candida albicans* biofilms, *Methods Mol. Med.* 118 (2005) 71-79. Doi: 10.1385/1-59259-943-5:071.

[8] L. Sherry, R. Rajendran, D.F. Lappin, E. Borghi, F. Perdoni, M. Falleni, D. Tosi, K. Smith, C. Williams, B. Jones, C.J. Nile, G. Ramage, Biofilms formed by *Candida albicans* bloodstream isolates display phenotypic and transcriptional heterogeneity that are associated with resistance and pathogenicity, *BMC Microbiol.* 14 (2014) 182. Doi: 10.1186/1471-2180-14-182.

[9] J.D. dos Santos, E. Piva, S.F. Vilela, A.O. Jorge, J.C. Junqueira, Mixed biofilms formed by *C. albicans* and non-*albicans* species: a study of microbial interactions, *Braz. Oral Res.* 30 (2016) e23. Doi: 10.1590/1807-3107BOR-2016.vol30.0023.

[10] C.J. Nobile, A.D. Johnson, *Candida albicans* biofilms and human disease, *Annu. Rev. Microbiol.* 69 (2015) 71-92. Doi: 10.1146/annurev-micro-091014-104330.

[11] M. Ghannoum, E. Roilides, A. Katragkou, V. Petraitis, T.J. Walsh, The role of echinocandins in *Candida* biofilm-related vascular catheter infections: *in vitro* and *in vivo* model systems, *Clin. Infect. Dis.* 61 (2015) S618-S621. Doi: 10.1093/cid/civ815.

[12] A.C. Mesa-Arango, A. Forastiero, L. Bernal-Martínez, M. Cuenca-Estrella, E. Mellado, O. Zaragoza, The non-mammalian host *Galleria mellonella* can be used to study the virulence of the fungal pathogen *Candida tropicalis* and the efficacy of antifungal drugs during infection by this pathogenic yeast, *Med. Mycol.* 51 (2013) 461-472. Doi: 10.3109/13693786.2012.737031.

[13] C.J. Tsai, J.M. Loh, T. Proft, *Galleria mellonella* infection models for the study of bacterial diseases and for antimicrobial drug testing, *Virulence* 7 (2016) 214-229. Doi: 10.1080/21505594.2015.1135289.

[14] J.M. Loh, N. Adenwalla, S. Wiles, T. Proft, *Galleria mellonella* larvae as an infection model for group A streptococcus, *Virulence* 4 (2013) 419-428. Doi: 10.4161/viru.24930.

[15] O.L. Champion, S. Wagley, R.W. Titball, *Galleria mellonella* as a model host for microbiological and toxin research, *Virulence* 7 (2016) 840-845. Doi: 10.1080/21505594.2016.1203486.

[16] M. Staniszewska, M. Bondaryk, M. Wieczorek, E. Estrada-Mata, H.M. Mora-Montes, Z. Ochal, Antifungal effect of novel 2-bromo-2-chloro-2-(4-chlorophenylsulfonyl)-1-

phenylethanone against *Candida* strains. *Front. Microbiol*. 7 (2016) 1309. Doi: 10.3389/fmicb.2016.01309.

[17] Clinical and Laboratory Standards Institute (CLSI). Reference method for broth dilution antifungal susceptibility testing of yeasts; approved standard-third edition, in: CLSI document M27-A3. Clinical and Laboratory Standards Institute, Wayne PA, USA, 2008.

[18] F.M. Garibotto, A.D. Garro, M.F. Masman, A.M. Rodríguez, P.G. Luiten, M. Raimondi, S.A. Zacchino, C. Somlai, B. Penke, R.D. Enriz, New small-size peptides possessing antifungal activity, *Bioorg. Med. Chem.* 18, (2010) 158-167. Doi: 10.1016/j.bmc.2009.11.009.

[19] C. Rueda, M. Cuenca-Estrella, O. Zaragoza, Paradoxical growth of *Candida albicans* in the presence of caspofungin is associated with multiple cell wall rearragements and decreased virulence, *Antimicrob. Agents Chemother.* 58 (2014) 1071-1083. Doi: 10.1128/AAC.00946-13.

[20] L. Majoros, G. Kardos, B. Szabó, M. Sipiczki, Caspofungin susceptibility testing of *Candida inconspicua*: correlation of different methods with the minima fungicidal concentration, *Antimicrob. Agents Chemother.* 49 (2005) 3486-3488. Doi: 10.1128/AAC.49.8.3486-3488.2005.

[21] M. Bondaryk, E. Łukowska-Chojnacka, M. Staniszewska, Tetrazole activity against *Candida albicans*. The role of *KEX2* mutations in the sensitivity to (±)-1-[5-(2-chlorophenyl)-2H-tetrazol-2-yl]propan-2-yl acetate, *Bioorg. Med. Chem. Lett.* 25 (2015) 2657-2663. Doi: 10.1016/j.bmcl.2015.04.078.

[22] M. Staniszewska, M. Bondaryk, M. Kazek, A. Gliniewicz, C. Braunsdorf, M. Schaller, H.M. Mora-Montes, Z. Ochal, Effect of serine pro tease *KEX2* on *Candida albicans* virulence under halogenated metyl sulfones, *Future Microbiol.* 12 (2017) 285-306. Doi: 10.2217/fmb-2016-0141.

[23] E. Łukowska-Chojnacka, J. Mierzejewska, M. Milner-Krawczyk, M. Bondaryk, M. Staniszewska, Synthesis of novel tetrazole derivatives and evaluation of their antifungal actitivy. *Bioorg. Med. Chem.* 24 (2016) 6058-6065. Doi: 10.1016/j.bmc.2016.09.066.

[24] M. Gulati, C.J. Nobile, *Candida albicans* biofilms: development, regulation, and molecular mechanisms, *Microbes Infect.* 18 (2016) 310-21. Doi: 10.1016/j.micinf.2016.01.002.

[25] A. P. Desbois, P. J. Coote, Wax moth larva (*Galleria mellonela*): an *in vivo* model for assessing the efficacy of antistaphylococcal agents, *J. Antimicrob. Chemother.* 66 (2011) 1785-1790. Doi: 10.1093/jac/dkr198.

[26] E. Movahed, G.M. Tan, K. Munusamy, T. C. Yeow, S.T. Tay, W.F. Wong, C.Y. Looi, Triclosan demonstrates synergic effect with amphotericin b and fluconazole and induces apoptosis-like cell death in *Cryptococcus neoformans*, *Front. Microbiol.* 7 (2016) 360. Doi: 10.3389/fmicb.2016.00360.

[27] S.P. Bachmann, K. VandeWalle, G. Ramage, T.F. Patterson, B.L. Wickes, J.R. Graybill, J. L. López-Ribot, *In vitro* activity of caspofungin against *Candida albicans* biofilms, *Antimicrob. Agents Chemother.* 46 (2002) 3591-3596. Doi: 10.1128/AAC.46.11.3591-3596.2002.

[28] G.B. Zore, A.D. Thakre, V. Rathod, S. M. Karuppayil, Evaluation of anti-*Candida* potential of geranium oil constituents against clinical isolates of *Candida albicans* differentially sensitive to fluconazole: inhibition of growth, dimorphism and sensitization, *Mycoses* 54 (2011) e99-e109. Doi: 10.1111/j.1439-0507.2009.01852.x.

[29] M. Staniszewska, M. Bondaryk, Z. Ochal, Polish Patent Application P.408765. July 4th, 2014.

[30] J.V. Pereira, I.A. Freires, A.R. Castilho, M.G. da Cunha, S. Alves Hda, P.L. Rosalen, Antifungal potential of *Sideroxylon obtusifolium* and *Syzygium cumini* and their mode of action against *Candida albicans*, *Pharm. Biol.* 55 (2016) 2312-2319. Doi: 10.3109/13880209.2016.1155629.

[31] P.l. Olive, J.P. Banáth, The comet assay: a method to measure DNA damage in individual cells, *Nat. Proc.* 1 (2006) 23-29, Doi: 10.1038/nprot.2006.5.

[32] S. Kasibhatla, G.P. Amarante-Mendes, D. Finucane, T. Brunner, E. Bossy-Wetzel, D.R. Green, Analysis of DNA fragmentation using agarose gel electrophoresis, *CSH Protoc.* 2006 (2006) pii: pdb.prot4429. Doi: 10.1101/pdb.prot4429.

[33] Y.R. Saadat, N. Saeidi, S.Z. Vaged, A. Barzegari, J. Barar, An update to DNA ladder assay for apoptosis detection, *Bioimpacts* 5 (2015) 25-28. Doi: 10.15171/bi.2015.01.

[34] P. Zielińska, M. Staniszewska, M. Bondaryk, M. Koronkiewicz, Z. Urbańczyk-Lipkowska, Design and studies of multiple mechanism of anti-*Candida* activity of a new Trp-rich peptide dendrimers, *Eur. J. Med. Chem.* 105 (2015) 106-119. Doi: 10.1016/j.ejmech.2015.10.013.

[35] W.G. Finnegan, R.A. Henry, R. Lofquist, An improved synthesis of 5-substituted tetrazoles, *J. Am. Chem. Soc.* 80 (1958) 3908-3911.

[36] T. Kimura, Y. Takase, K. Hayashi, H. Tanaka, I. Ohtsuka, T. Saeki, M. Kogushi, T. Yamada, T. Fujimori, Structure-activity relationship of N-[[2-(dimethylamino)-6-[3-(5-methyl-4-phenyl-1H-imidazol-1-yl)propoxy]phenyl]-N'-pentylurea and analogs. Novel potent

inhibitors of acyl-CoA:cholesterol O-acyltransferase with antiatherosclerotic activity, *J. Med. Chem.* 36 (1993) 1630-1640. Doi: 10.1021/jm00063a013.

[37] R. A. Henry, R.A. Methylation of 5-phenyltetrazole, *J. Am. Chem. Soc.* 73 (1951), 73, 4470-4470.

[38] E. Łukowska-Chojnacka, P. Wińska, M. Wielechowska, M. Bretner, Synthesis of polybrominated benzimidazole and benzotriazole derivatives containing a tetrazole ring and their cytotoxic activity, *Monatsh Chem.* 147 (2016) 1789-1796. Doi: 10.1007/s00706-016-1785-8.

[39] I. Unal Cevik, T. Dalkara, Intravenously administered propidium iodide labels necrotic cells in the intact mouse brain after injury, *Cell Death Differ.* 10 (2003) 928-929. Doi: 10.1038/sj.cdd.4401250.

[40] S.A. Rostom, H.M. Ashour, H.A. El Razik, A.F. Eifattah, N.N. El-din, Azole antimicrobial pharmacophore-based tetrazoles: synthesis and biological evaluation as potential antimicrobial and anticonvulsant agents, *Bioorg. Med. Chem.* 17 (2009) 2410-2422. Doi: 10.1016/j.bmc.2009.02.004.

[41] M.A. Malik, S.A. Al-Thabaiti, M.A. Malik, Synthesis, structure optimization and antifungal screening of novel tetrazole ring bearing acyl-hydrazones, *Int. J. Mol. Sci.* 13 (2012) 10880-10898, Doi: 10.3390/ijms130910880.

[42] S. Kanakaraju, P. Sagar Vijay Kumar, B. Prasanna, G.V. Chandramouli, Design, synthesis, and in vitro antimicrobial evaluation of fused pyrano[3,2-e]tetrazolo[1,5-c]pyrimidines and diazepines, *ISRN Org. Chem.* 2013 (2013) 635384. Doi: 10.1155/2013/635384.

[43] L.V. Kumar, P.J. Naik, M. Naveen, T. Chandrasekhar, A.B. Reddy, Synthesis and biological evaluation of some new 2,5-disubstituted 1,3,4-oxidiazoles from 3-(arylsulfonyl) propanehydrazides, *Indian J. Chem.* 53B (2014) 208-211.

[44] C. Kragelund, Exploiting new knowledge of candidal infection for future antifungal combat, *Oral Dis.* 23 (2017) 543-547. Doi: 10.1111/odi.12546.

[45] T.Y. Kalhor-Monfared, Z. Wawrzak, D.C. Lamb, F.P. Guengerich, G.I. Lepesheva, Structure-functional characterization of cytochrome P450 sterol 14α-demethylase (CYP51B) from *Aspergillus fumigatus* and molecular basis for the development of antifungal drugs, *J. Biol. Chem.* 290 (2016) 23916-23934. Doi: 10.1074/jbc.M115.677310.

[46] T.Y. Hargrove, L. Friggeri, Z. Wawrzak, A. Qi, W.J. Hoekstra, R.J. Schotzinger, J.D. York, F.P. Guengerich, G.I. Lepesheva, Structural analyses of *Candida albicans* sterol 14α-demethylase complexed with azole drugs address the molecular basis of azole-mediated

inhibition of fungal sterol biosynthesis, *J. Biol. Chem.* 292 (2017) 6728-6743. Doi: 10.1074/jbc.M117.778308.

[47] E.P. Garvey, W.J. Hoekstra, R.J. Schotzinger, J.D. Sobel, E.A. Lilly, P.L. Fidel Jr., Efficacy of the clinical agent VT-1161 against fluconazole-sensitive and –resistant *Candida albicans* in a murine model of vaginal candidiasis, *Antimicrob. Agents Chemother.* 59 (2015) 5567-5573. Doi: 10.1128/AAC.00185-15.

[48] L.S. Shubitz, H.T. Trinh, J.N. Galgiani, M.L. Lewis, A.W. Fothergill, N.P. Wiederhold, B.M. Barker, E.R.G.Lewis, A.L. Doyle, W.J. Hoekstra, R.J. Schotzinger, E.P. Garvey, Evaluation of VT-1161 for treatment of coccidioidomycosis in murine infection models, *Antimicrob. Agents Chemother.* 59 (2015) 7249-7254.

[49] S.R. Lockhart, A.W. Fothergill, N. Iqbal, C.B. Bolden, N.T. Grossman, E.P. Garvey, S.R. Brand, W.J. Hoekstra, R.J. Schotzinger, E. Ottinger, T.F. Patterson, N.P. Wiederhold, The investigational fungal Cyp51 inhibitor VT-1129 demonstrates potent *in vitro* activity against *Cryptococcus neoformans* and *Cryptococcus gattii*, *Antimicrob. Agents Chemother.* 60 (2015) 2528-2531. Doi: 10.1128/AAC.02770-15.

[50] J.A. Parente-Rocha, A.M. Bailão, A.C. Amaral, C.P. Taborda, J.D. Paccez, C.L. Borges, M. Pereira, Antifungal resistance, metabolic routes as drug targets, and new antifungal agents: an overview about endemic dimorphic fungi, *Mediators Inflamm.* 2017 (2017) 9870679. Doi: 10.1155/2017/9870679.

[51] N. Matsumori, Y. Sawada, M. Murata, Mycosamine orientation of amphotericin B controlling interaction with ergosterol: sterol-dependent activity of conformation-restricted derivatives with an amino-carbonyl bridge, *J. Am. Chem. Soc.* 127 (2005) 10667-10675. Doi: 10.1021/ja051597r.

[52] G. Banfalvi, Methods to detect apoptic cell death, *Apoptosis* 22 (2017) 306-323. Doi: 10.1007/s10495-016-1333-3.

[53] N. Atale, S. Gupta, U.C.S. Yadav, V. Rani, Cell-death assessment by fluorescent and nonfluorescent cytosolic and nuclear staining techniques, *J. Microsc.* 255 (2014) 7-19. Doi: 10.1111/jmi.12133.

[54] K. Liu, P.C. Liu, R. Liu, X. Wu, Dual AO/EB staining to detect apoptosis in osteosarcoma cells compared with flow cytometry, *Med. Sci. Monit. Basec Res.* 21 (2015) 15-20. Doi: 10.12659/MSMBR.893327.

[55] J. Světlík, A. Martvoň, J. Leško, Preparation and spectral properties of tetrazoles, *Chem. Pap.* 33 (1979) 521-527.

[56] O. Marchetti, P. Moreillon, M.P. Glauser, J. Bille, D. Sanglard, Potent synergism of the combination of fluconazole and cyclosporine in *Candida albicans*, *Antimicrob. Agents Chemother.* 44 (2000) 2373-2381.

[57] A. Escalante, M. Gattuso, P. Pérez, S. Zacchino, Evidence for the mechanism of action of the antifungal phytolaccoside B isolated from *Phytolacca tetramera* Hauman, *J. Nat. Proc.* 71 (2008) 1720-1725. Doi: 10.1021/np070660i.

[58] Z. Darzynkiewicz, S. Bruno, G. Del Bino, W. Gorczyca, M.A. Hotz, P. Lassota, F. Traganos, Features of apoptic cells measured by flow cytometry, *Cytometry* 13 (1992) 795-808. Doi: 10.1002/cyto.990130802.

[59] L. Scorzoni, M.P. de Lucas, A.C. Mesa-Arango, A.M. usco-Almeida, E. Lozano, M. Cuenca-Estrella, M.J. Mendes-Giannini, O. Zaragoza, Antifungal efficacy during *Candida krusei* infection in non-conventional models correlates with the yeast *in vitro* susceptibility profile, *PLoS One* 8 (2013) e60047. Doi: 10.1371/journal.pone.0060047.

Bullet points:

- **2d** targets to the *C. albicans* cell wall and attenuates morphogenesis in mature biofilm;
- **6a** induces DNA denaturation, mitochondrial damage, and reduces adhesion to human epithelium;
- **2d** and **6a**, generate necrosis of the *C. albicans'* biofilm, without toxicity *in vitro* and *in vivo.*